SRNL-STI-2011-00546
Revision 0

Computer Modeling of High-Level Waste Glass Temperatures Within DWPF Canisters During Pouring and Cool Down

J.W. Amoroso

September 2011

Savannah River National Laboratory
Savannah River Nuclear Solutions, LLC
Aiken, SC 29808

Prepared for the U.S. Department of Energy under contract number DE-AC09-08SR22470.

SRNL
SAVANNAH RIVER NATIONAL LABORATORY
TM

DISCLAIMER

Printed in the United States of America

Prepared for
U.S. Department of Energy

SRNL-STI-2011-00546
Revision 0

Keywords: *Nepheline, CCC , Crystallization, DWPF*

Retention: *Permanent*

Computer Modeling of High-Level Waste Glass Temperatures Within DWPF Canisters During Pouring and Cool Down

J.W. Amoroso

September 2011

Savannah River National Laboratory
Savannah River Nuclear Solutions, LLC
Aiken, SC 29808

Prepared for the U.S. Department of Energy under contract number DE-AC09-08SR22470.

SRNL
SAVANNAH RIVER NATIONAL LABORATORY
TM

REVIEWS AND APPROVALS

AUTHOR:

J.W. Amoroso, Process Technology Programs Date

TECHNICAL REVIEW:

F. C. Johnson, Process Technology Programs Date

APPROVALS:

C. C. Herman, Manager Date
Process Technology Programs

S.L. Marra, Manager Date
Environmental & Chemical Process Technology Research Programs

ACKNOWLEDGEMENTS

The author would like to thank Matt Kesterson at the Savannah River National Laboratory (SRNL) for developing the model, generating the data, and help interpreting the data used in this report. The author acknowledges the U.S. Department of Energy Office of Environmental Management for financial support of this work.

EXECUTIVE SUMMARY

This report describes the results of a computer simulation study to predict the temperature of the glass at any location inside a DWPF canister during pouring and subsequent cooling. These simulations are an integral part of a larger research focus aimed at developing methods to predict, evaluate, and ultimately suppress nepheline formation in HLW glasses. That larger research focus is centered on holistically understanding nepheline formation in HLW glass by exploring the fundamental thermal and chemical driving forces for nepheline crystallization with respect to realistic processing conditions. Through experimental work, the goal is to integrate nepheline crystallization potential in HLW glass with processing capability to ultimately optimize waste loading and throughput while maintaining an acceptable product with respect to durability.

The results of this study indicated severe temperature gradients and prolonged temperature dwell times exist throughout different locations in the canister and that the time and temperatures that HLW glass is subjected to during processing is a function of pour rate. The simulations indicate that crystallization driving forces are not uniform throughout the glass volume in a DWPF (or DWPF-like) canister and illustrate the importance of considering overall kinetics (chemical and thermal driving forces) of nepheline formation when developing methods to predict and suppress its formation in HLW glasses.

The intended path forward is to use the simulation data both as a driver for future experimental work and, as an investigative tool for evaluating the impact of experimental results. Simulation data will be used to develop laboratory experiments to more acutely evaluate nepheline formation in HLW glass by incorporating the simulated temperatures throughout the canister into the laboratory experiments. Concurrently, laboratory experiments will be performed to identify nepheline crystallization potential in HLW glass as a function of time and temperature, the results of which will be fed back into simulations to evaluate the potential impacts. Through an iterative process involving computer simulations and experimental results, the potential for nepheline crystallization in HLW glass can be predicted, evaluated, and suppressed to maximize waste loading and throughput of canisters.

TABLE OF CONTENTS

LIST OF TABLES

LIST OF FIGURES

LIST OF ABBREVIATIONS

CCC	Canister Centerline Cooling
DWPF	Defense Waste Processing Facility
g	Gram (s)
HLW	High Level Waste
ND	Nepheline Discriminator
PCT	Product Consistency Test
PNNL	Pacific Northwest National Laboratory
SGM	Scale Glass Melter
SRNL	Savannah River National Laboratory

1.0 Introduction

Currently, the Nepheline Discriminator (ND), a constraint developed by Pacific Northwest National Laboratory (PNNL)[1] is used to prevent nepheline crystallization in HLW glass at the Defense Waste Processing Facility (DWPF)[2]. The current ND is a purely compositional constraint[a] although it is well known that crystallization in glasses is controlled by kinetics factors as well. In glasses, the kinetic, or rates of mass transport, driving forces for crystallization can be explained in reference to the glass transition region. Unlike crystalline materials which undergo instantaneous[b] bulk crystallization upon cooling below the melting temperature, glasses undergo what is termed a glass transition[c] in which the solidification occurs over a longer period of time and temperature.[d] Therefore, glasses that are cooled at different rates will have different kinetic driving forces for crystallization and thus different amounts of crystallization. This knowledge was the basis for developing the canister centerline cooling (CCC) heat treatment test as part of the waste form compliance plan.[3,4] The CCC test is a laboratory crucible test in which glass is heat treated according to a schedule intended to mimic a "worst-case" kinetic scenario based on the slowest measured cooling rate.[3,5] Indeed, it has been shown that kinetic effects exist and impact the measured nepheline crystallization in HLW glass.[6] As a result, experimental studies at SRNL are ongoing to understand the impact of kinetics on nepheline crystallization and to develop improved methods of preventing nepheline crystallization in HLW glass during processing.

Computer simulations have been performed as part of a larger motivation to holistically understand nepheline formation in high-level-nuclear waste (HLW) glasses. The reason for this is that in order to meet projected increased waste loadings in the future, particularly for waste high in sodium and aluminum, the current nepheline constraint, the ND), will likely need to be modified. In fact, projected waste loadings will likely not be achieved for the high Al-waste streams to be vitrified at Hanford or Savannah River without modifying the current ND or implementing a supplemental constraint. Therefore, Savannah River National Laboratory (SRNL) has been researching methods and ways to better predict and limit nepheline crystallization in HLW glass.

This report details computer simulations developed to model the temperatures of the glass within a DWPF canister during filling and cooling. This research is focused on the kinetics of nepheline crystallization and therefore the temperatures of the glass throughout the canister were of primary importance. A realistic working computer model of the canister filling process was developed so that changes to the process parameters (pour rate, heat flow, melt temperature, etc.) or glass properties (density, viscosity, etc.) could be simulated, and the impacts to the glass temperatures inside the canister identified, without actually or experimentally filling a canister. Ultimately, the computer simulations will be used in two ways; (1) to drive future experiments for predicting nepheline crystallization and (2) to investigate or identify those portions of the glass inside a canister which are prone to nepheline crystallization given compositional *and* kinetic factors.

[a] Although the ND was developed based on glasses that were subjected to a variety of slow cooling profiles, the ND as it is used/defined does not include (nor require) a cooling rate term.
[b] The transition is not actually instantaneous but, the kinetics is generally orders of magnitude faster compared to glasses such that the liquid solidifies over an extremely small temperature range. In fact, it is now recognized that any material can be frozen into a glassy state if cooled at a sufficiently fast rate.
[c] The glass transition is the range of temperatures over which the supercooled liquid remains liquid-like and its viscosity increases as temperature decreases until the glass transition temperature where the viscosity is sufficiently ($\sim 10^{12}$ Pa-s) high that the glass becomes rigid.
[d] In fact, it is now recognized that any material can be "frozen" into a glassy state if cooled at a sufficiently fast rate to overcome the kinetics of mass transport.

In order for (2) to be most beneficial, crystallization[a] studies are first needed to identify the time-temperature (kinetic) conditions in which nepheline crystallization is most probable in HLW glasses. The crystallization experiments will involve using thermal analysis measurements to identify nucleation and crystal growth rates as a function of temperature.[7] Then, by comparing the simulated temperatures of the glass in the canister to the temperatures at which nepheline nucleation and crystal growth occurs, portions of the glass within the canister that are at increased risk to nepheline crystallization can be identified. The simulations presented in this report are the first step in developing a more robust and complete method for predicting nepheline crystallization in HLW glass than currently available.

This study was performed for the Department of Energy (DOE) Office of Environmental Management (EM) under the Technology Development and Deployment (TDD) Program Task Plan EM-31 WP-5.1.2.[8] This report is intended to support the deliverable WP-512-SRNL-02 as identified in the Task Plan.

[a] Crystallization refers to both nucleation and crystal growth, both of which are required for crystallization.

2.0 Experimental

2.1 Model Development

The details of the computer model and its input parameters used to generate the data in this report are described in detail in report SRNL-STI-2011-00209, Rev. 1.[9] In brief, this model was developed in part by using known thermal property data for nuclear waste glass and comparing the model output temperatures to measured thermocouple data obtained during scale glass melter (SGM) runs.[3,10] In developing this model it was necessary that the glass pour rate be an adjustable input parameter, however, because the thermal conductivity for a typical HLW glass was not known, the heat conduction term in the model could not be developed from the thermal equations alone. Instead, a flow rate calculation as the glass stream enters the glass pool inside the canister was used to model the heat conduction as a function of radial distance from the center, similar to that developed by Tennant.[11] The heat conduction inputs were based on the initial model simulations developed to fit experimental data.[10] The model simulation and the experimental data were in good agreement. The trends observed in the experimental data were reproducible and the largest temperature difference between the simulation and experimental data was ~40 °C. Although the model used in these simulations was developed to approximate the heat flow, since it was developed from a single experimental data set[10] there is little ability to verify the accuracy of the simulations for the various pour rates. Additional SGM runs with experimental thermocouple data exist in the literature for batch pours and continuous pours.[3,12] However, the batch pour data was not used in the model development because DWPF targets a continuous pour. Additionally, the available historical data for continuously poured canisters was generated using a narrow range in nominal pour rate (between 204 and 243 lbs./hr.)[3,12] insufficient for comparison purposes. Nevertheless, because of how the model simulates heat flow in the system, the overall trends seen in the data are thought to be accurate.

It should be understood that during processing the target pour rate of a given canister at DWPF will fluctuate. In addition, it is common practice for DWPF to increase the pour rate as the canister is nearly filled to lower the level in the melter in order to accommodate the incoming feed and maintain and adequate level in the melter during the time it takes to replace the filled canister with an empty canister.[13] The initial model development incorporated these flow rate fluctuations into the simulation by extrapolating flow rates from the experimental data (based on maximum thermocouple readings versus time) and increasing the pour rate for the last 100 lbs. of glass to be poured. For all of the experimental simulations in this study, the pour rate of the glass into the canister was held constant (except where intentionally varied) to simplify comparisons among simulations.

It is critical to recognize that the simulation operates by filling a canister along its centerline and allowing the glass to flow radially outward to the inside edge of the canister. Therefore, the centerline location reaches the highest temperature for a given height compared to the other radial distances. Furthermore, if the additional heat added to the system from an infinitesimal height increase in glass level[a] is negligible, then the maximum temperature of the centerline position at a particular height corresponds to the point (and associated time) at which the glass level reaches this height. Thus, the temperature of the *glass* at a particular height and radial position in the canister can be traced as a function of time from when the glass fills to that particular height until the end of the pour. By using this technique, the cooling curve profiles presented in this report could be generated.

[a] The temperature of the bottom of the glass stream increases as the glass height in the canister increases since the distance traveled is less.

2.2 Test Simulations Selection & Development

All simulations were performed by M. R. Kesterson using COMSOL[14] software. Eleven simulations were run in this study and they can be grouped into three categories; (1) continuous constant pour rate, (2) continuous non-constant pour rate, and (3) non-continuous pour rate. A 'baseline' simulation was run with a 228 lbs. of glass/hr. pour rate which, is equivalent to the DWPF target of 400 canisters per year[15] assuming approximately 4000 lbs. of glass per canister and 80% attainment at DWPF. To match the experimental data, for all simulations the actual fill height was approximately 92.1 inches which equated to approximately 3,656 pounds of glass.[a]

2.2.1 *Continuous Constant Pour Rate*

In addition to the baseline simulations, pour rates of 119 lbs./hr., 328 lbs./hr., and 470 lbs./hr. were also simulated. The increased pour rates, relative to the baseline, were simulated in anticipation of increased canister throughput goals. Although pour rates of 470 or 119 lbs./hr. are unlikely to be realized at DWPF, these simulations were meant to "bound" the anticipated pour rates used during DWPF processing and thereby "bound" the temperatures and dwell times (at temperatures) of the glass throughout the canister. These four simulations were performed to mimic a continuously fed canister at a constant rate. Figure 2-1 schematically shows these fill cycle profiles.

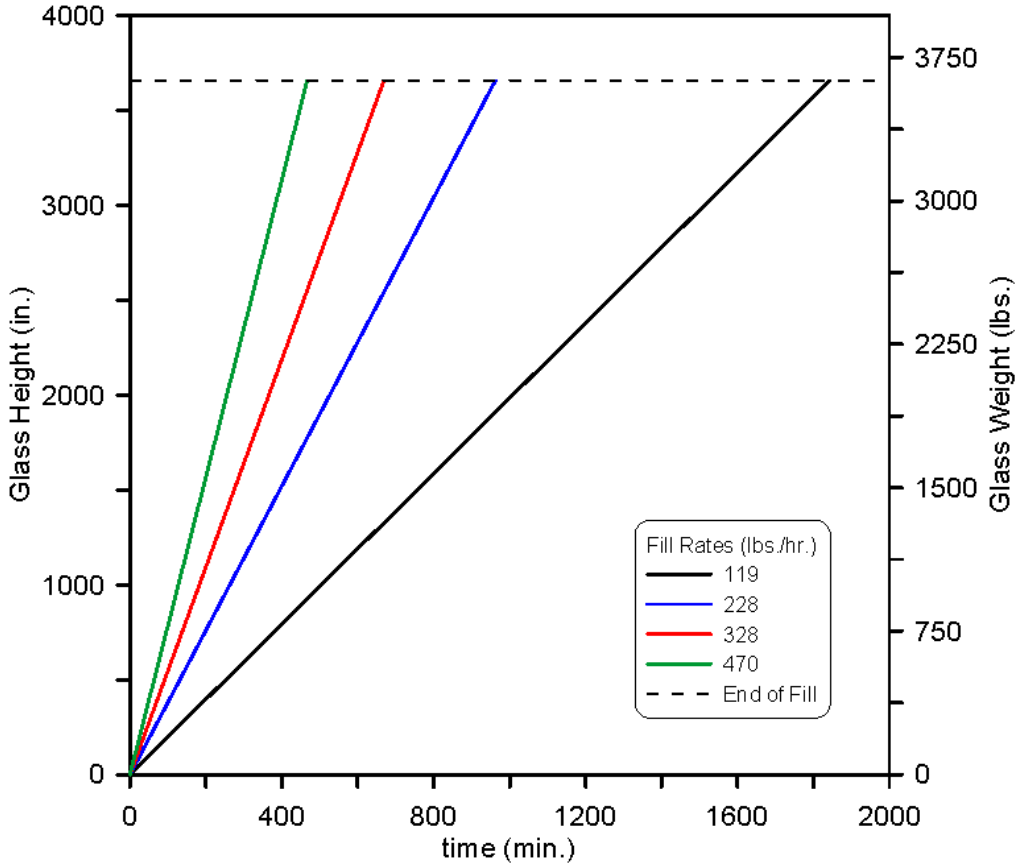

Figure 2-1. Fill cycles for constant pour rate simulations.

[a] Approximate density of 2.68 g/cc (167 lbs./ft^3).

2.2.2 *Continuous Non-Constant Pour Rate*

During actual processing the target pour rate for a given canister at DWPF will fluctuate. Therefore, four simulations were performed to mimic either increasing or decreasing the pour rate during the fill cycle with respect to the baseline. To facilitate comparison, the transition between pour rates was at 50% of the fill height for all simulations. The following pour rate transitions were simulated: 128 lbs./hr.→228 lbs./hr., 228 lbs./hr.→128 lbs./hr., 228 lbs./hr.→328 lbs./hr., and 328 lbs./hr.→228 lbs./hr. These pour schedules are referred to as 128-228, 228-128, 228-328, and 328-228 respectively and are shown graphically in Figure 2-1.

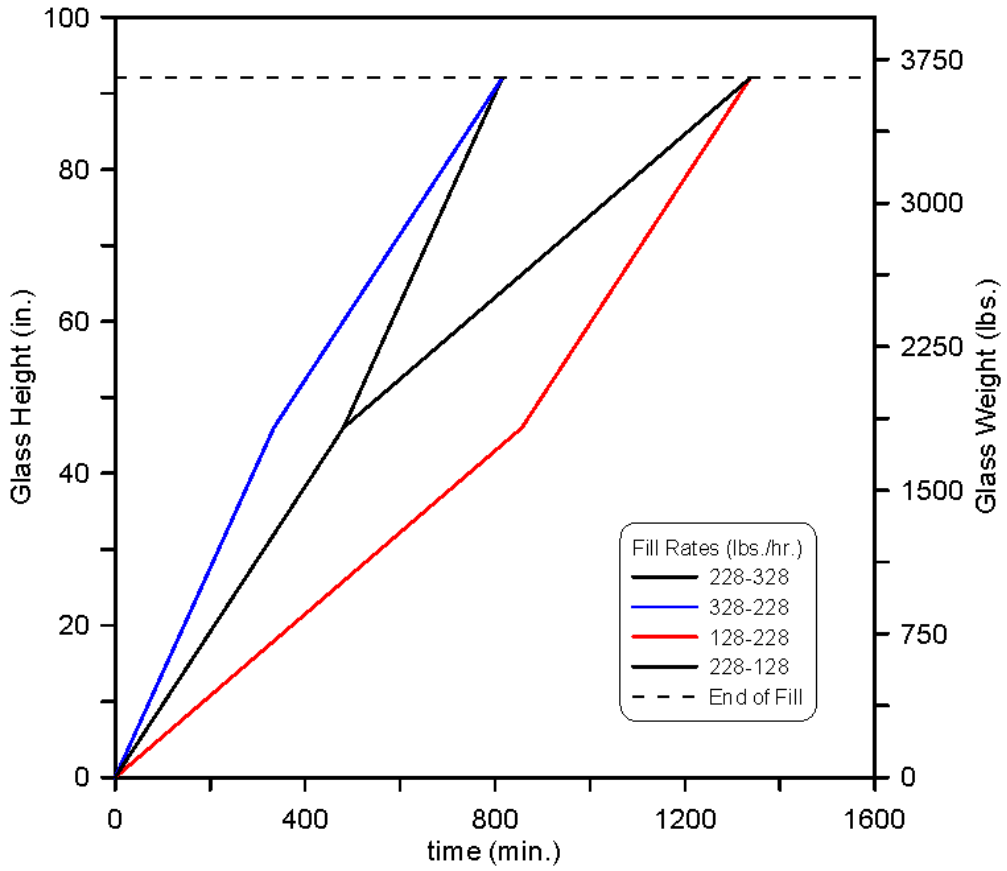

Figure 2-2. Fill cycles for on-constant pour rate simulations.

2.2.3 *Non-Continuous Pour Rate*

In addition to pour rate fluctuations, real process delays or interruptions can and have occurred when filling a given canister. To model these effects, three simulations were run in which filling was stopped and restarted. Two of these simulations were meant to mimic a full pour stop lasting one day (or long enough for the glass to cool to near room temperature). These simulations were run at a nominal pour rate of 228 lbs./hr. and the stops were initiated at 25% of the glass height in one simulation and at 75% of the glass height in the other simulation. In both cases the fill cycle was completed at the nominal 228 lbs./hr. after the glass inside the canister had cooled to near room temperature. These simulations are referred to in the text as "25/75" and "75/25" respectively. The last simulation used a series of stops and restarts to the pour during the fill cycle. In this simulation 100 lbs. of glass was poured at a nominal 228 lbs./hr. followed by a 60 minute hold. Immediately following the hold the same pour/hold sequence was repeated. In that fashion a stepwise incremental pour was continued until the canister was filled. This simulation

is referred to as "Step Flow (228/60)" in the text. Figure 2-3 schematically shows these non-continuous fill cycle profiles.

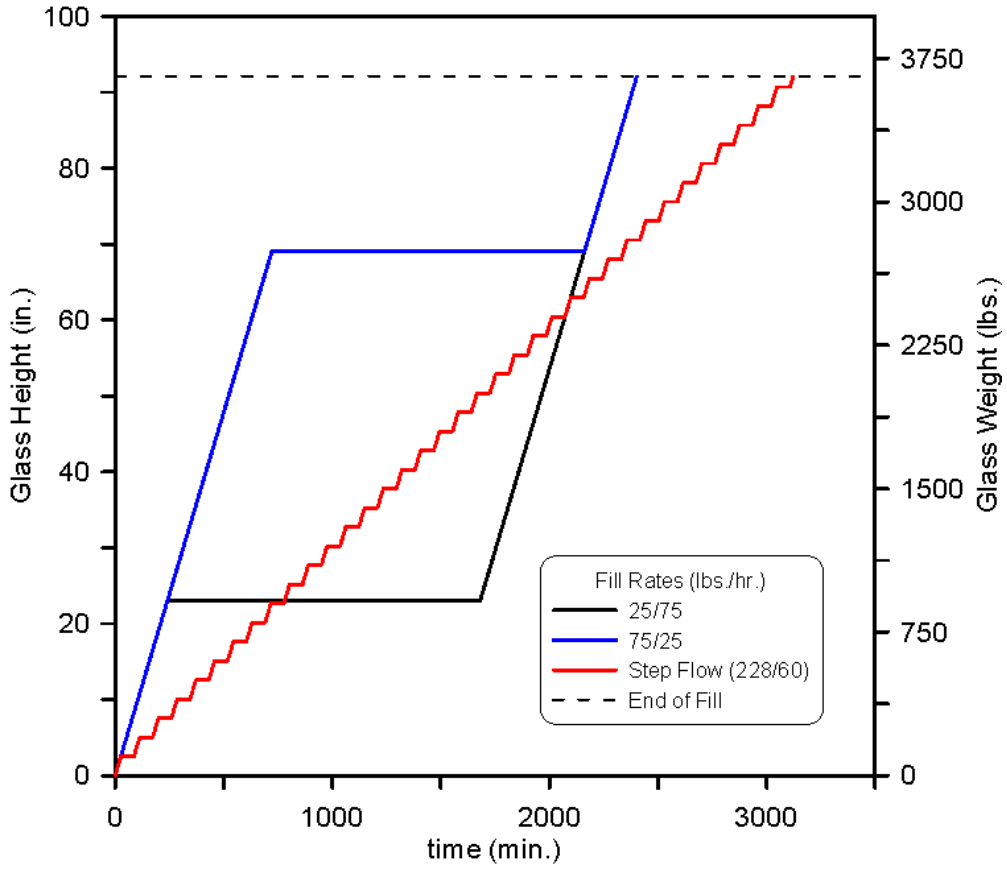

Figure 2-3. Fill cycles for non-continuous pour simulations

2.3 Data Output and Analysis

After running a simulation it was possible to extract the temperature of any location within the canister. However, for simplicity, in this work, two types of data output were analyzed: (1) radial temperature data and (2) temperature dwell charts.

2.3.1 *Radial Temperature Data*

The radial temperature data refers to six radial distances, 0", 1", 3", 6", 9", and 12" within a canister cross-section where the 0" location is the center of the canister and the 12" location is the interface between the glass and the internal canister wall. The temperature of these six radial distances, at five vertical heights, 15", 33", 51", 69", and 87" were extracted from each simulation as a function of time. All the radial distances and the 15", 51", and 87" vertical height locations were chosen because those locations are identical to the thermocouple locations in the experimental data.[3,10] The additional 33" and 69" vertical height locations were chosen because they were midway points between the other vertical height locations. These locations are shown schematically in Figure 2-4.

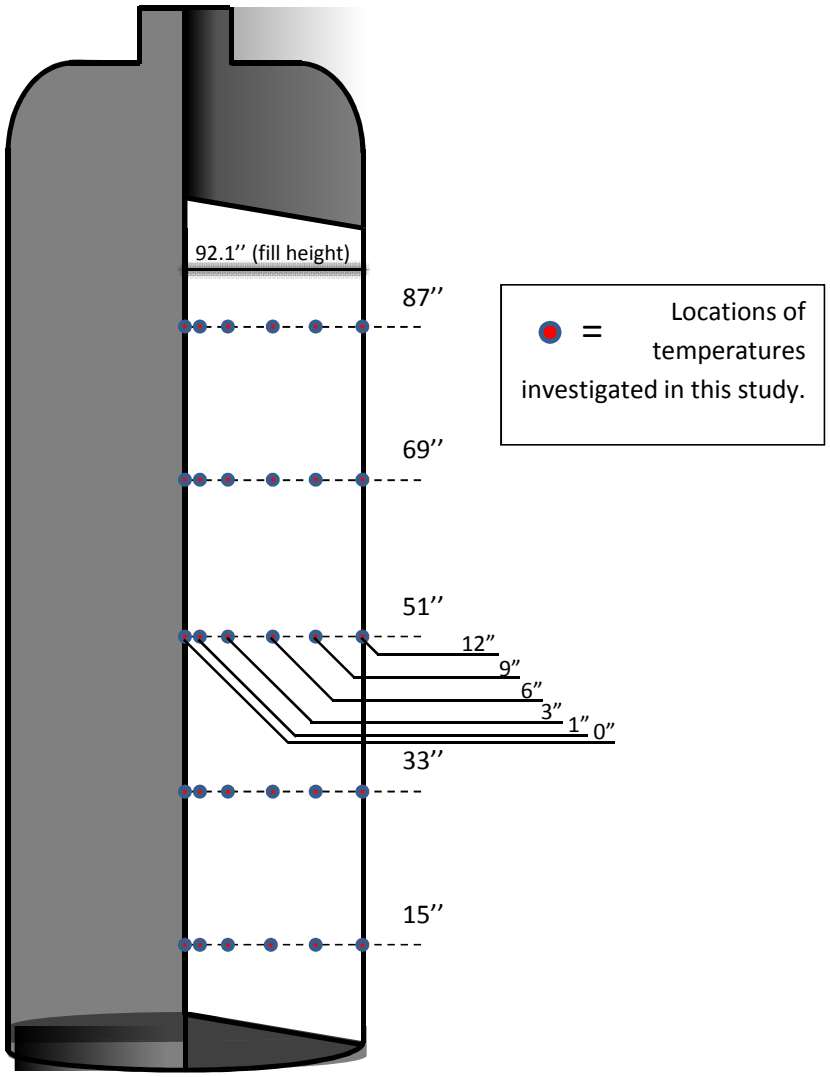

Figure 2-4. Schematic of a canister cross-section with radial distances and vertical heights investigated in this research labeled.

2.3.2 *Temperature Dwell Charts*

As previously mentioned, a focus of this research is to ultimately relate the simulated temperature profiles to nucleation and crystallization kinetics as they relate to nepheline formation. To that end, time-temperature dwell charts were generated with the intention of identifying locations within the total glass volume in which the temperature remains at or near nucleation/crystallization temperatures for extended periods of time. Previous literature has shown that nepheline forms in HLW waste at temperatures as low as 600 °C and as high as 1100 °C.[16,17] Therefore, the temperature regions chosen for analysis were 1100–1000 °C, 1000–900 °C, 900–800 °C, 800–700 °C, and 700–600 °C. These charts display the total time that any portion of the glass volume remained within a pre-determined temperature range. These charts had the benefit of displaying the entire glass volume in one chart but, the charts had to be generated during the simulations and therefore it was not possible to generate additional charts for different temperature ranges post-simulation. The gradient time-temperature charts were generated by the COMSOL software.[14]

3.0 Results and Discussion

3.1 Radial Temperature Data

To aid in interpreting the simulated radial temperature data it is helpful for the reader to recall how the canister is filled in the simulations (see Section 2.1). In particular, the simulated temperature at a given height and radial distance represents both the temperature of the air space before the glass level reaches said height and, subsequently, the temperature of the glass after the glass level has reached said height. In addition, for any simulation, the point in time at which the glass reaches a specified height can be extrapolated from the simulation by finding the maximum temperature at that height. By putting these two concepts together, it is trivial to separate the temperature of the *glass* from the temperature of the *air space* in the simulation data.

Two sets of radial temperature data are provided. Each set is comprised of five individual plots corresponding to the five vertical height locations (15", 33", 51", 69", and 87") in the canister. In each one of those plots, the temperatures as a function of time for the six radial distances are overlaid (0", 1", 3", 6", 9", and 12"). The first set, provided in Appendix A, shows the temperature of the glass *and* the air space within the canister at any time during the simulations. These plots are provided mostly for comparison purposes to show differences in simulation durations and also to show the temperature differences within the canister (air space) for each simulation. However, since the *glass* temperature was of primary interest, the second set of radial temperature data is provided in Figure 3-1 through Figure 3-11 that shows only the temperature of the glass. In this set, the same data (as shown in Appendix A) have been truncated along the x-axes (time) so that the origin corresponds to the maximum temperature (extrapolated from the simulation data as described above) of the centerline position at a given height or, more explicitly, once the glass level has reached the specified canister height. In these plots, two common characteristics are apparent.

First, the glass temperature, as a function of time, (cooling) was comparable for all the simulations and exhibited three slope (rate) changes; an initial rapid cooling rate that transitioned into a slower cooling rate before increasing again and transitioning into a cooling curve typical of conduction in an infinite solid.[18] A notable exception to this observation was the Step Flow (228/60) simulation however, this simulation also appeared to undergo similar cooling behavior albeit with a 'perturbed' cooling rate.

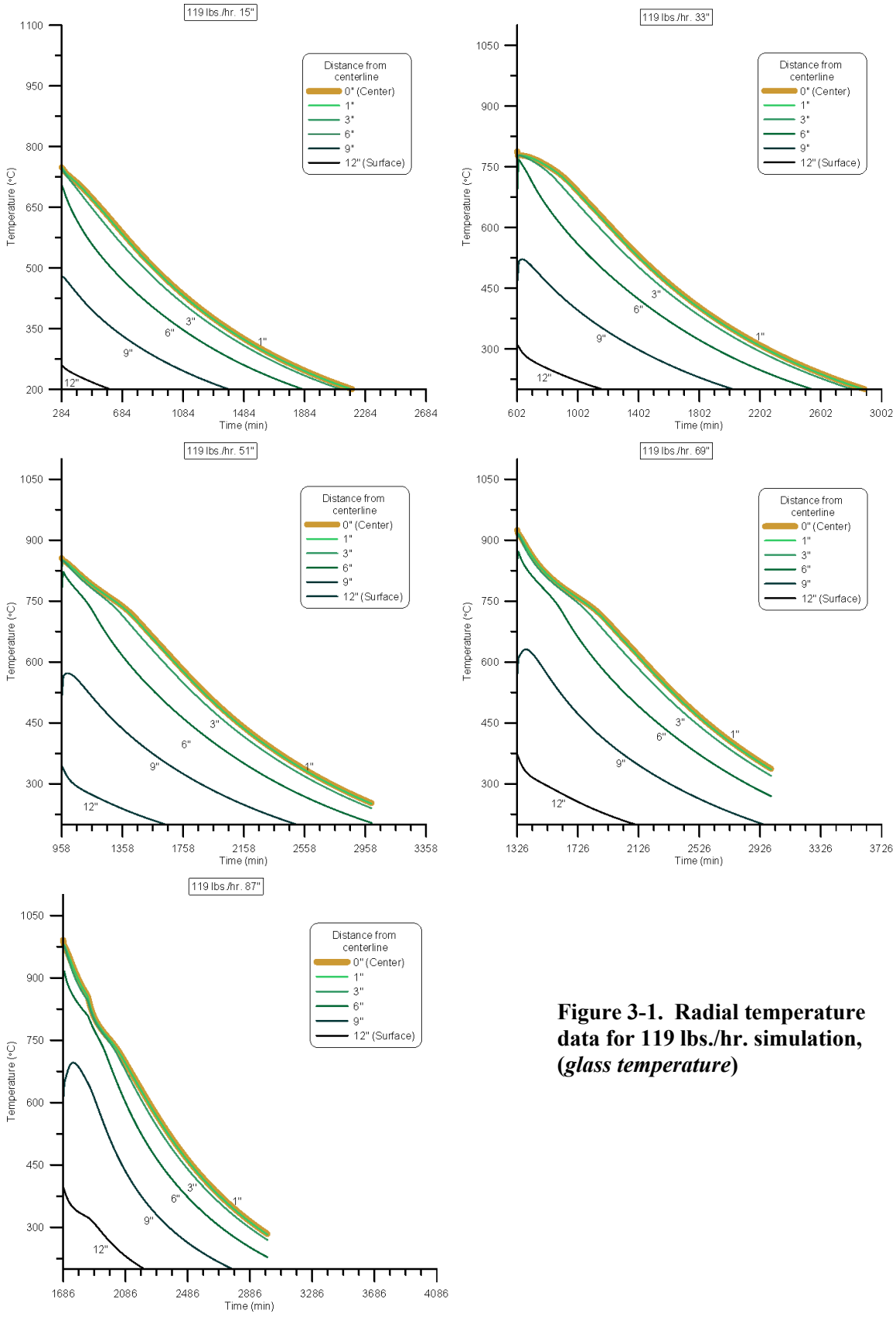

Figure 3-1. Radial temperature data for 119 lbs./hr. simulation, (*glass temperature*)

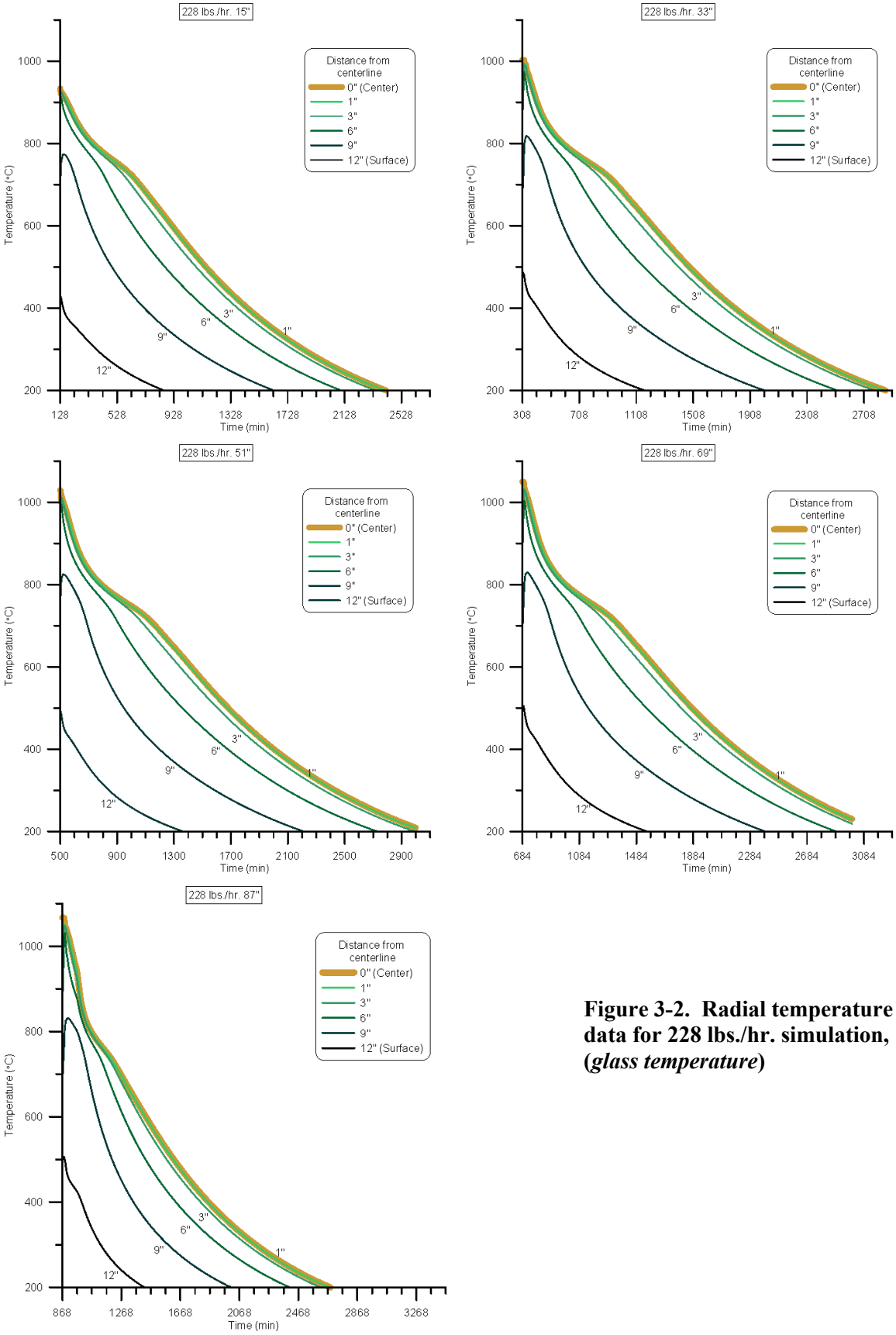

Figure 3-2. Radial temperature data for 228 lbs./hr. simulation, (*glass temperature*)

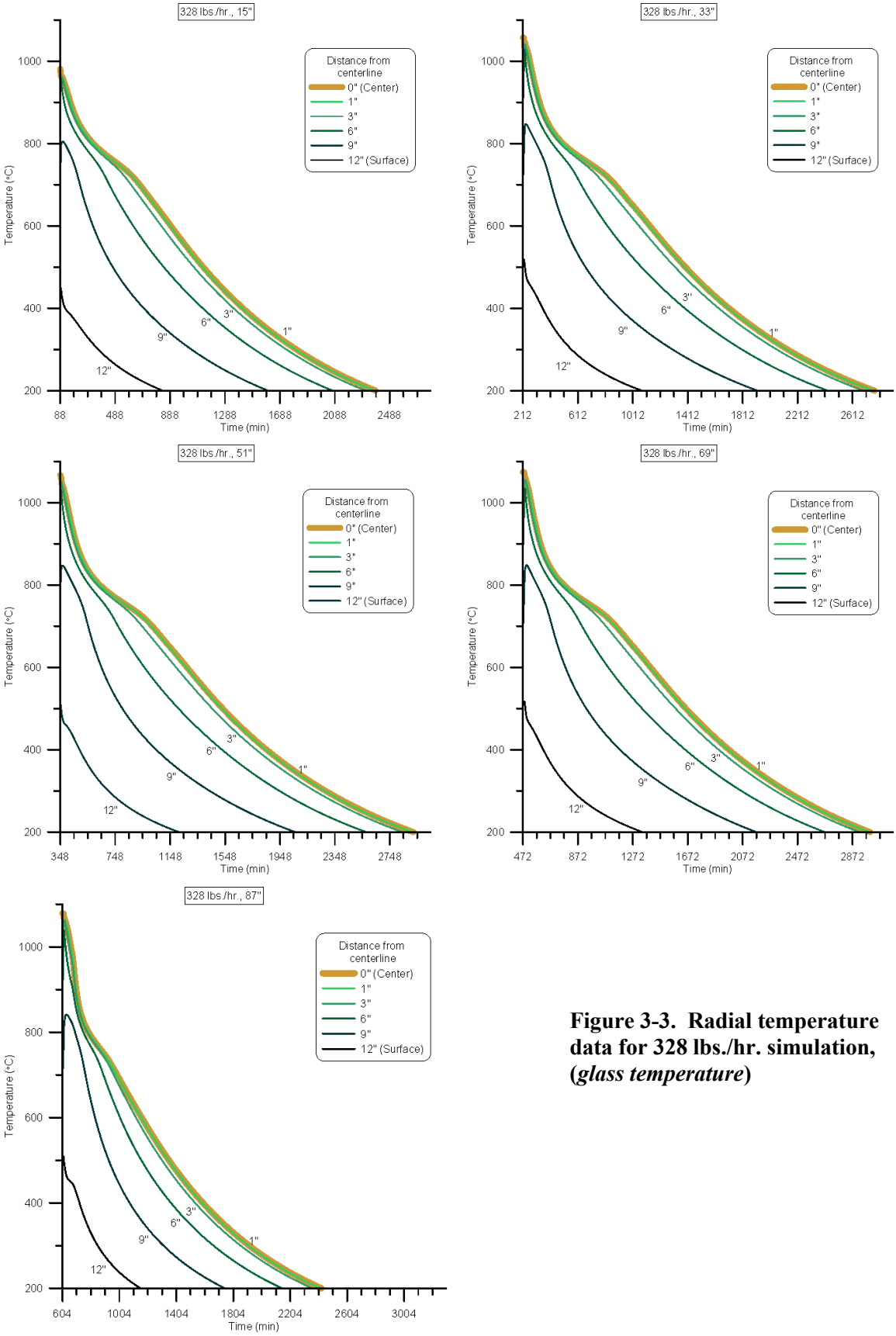

Figure 3-3. Radial temperature data for 328 lbs./hr. simulation, (*glass temperature*)

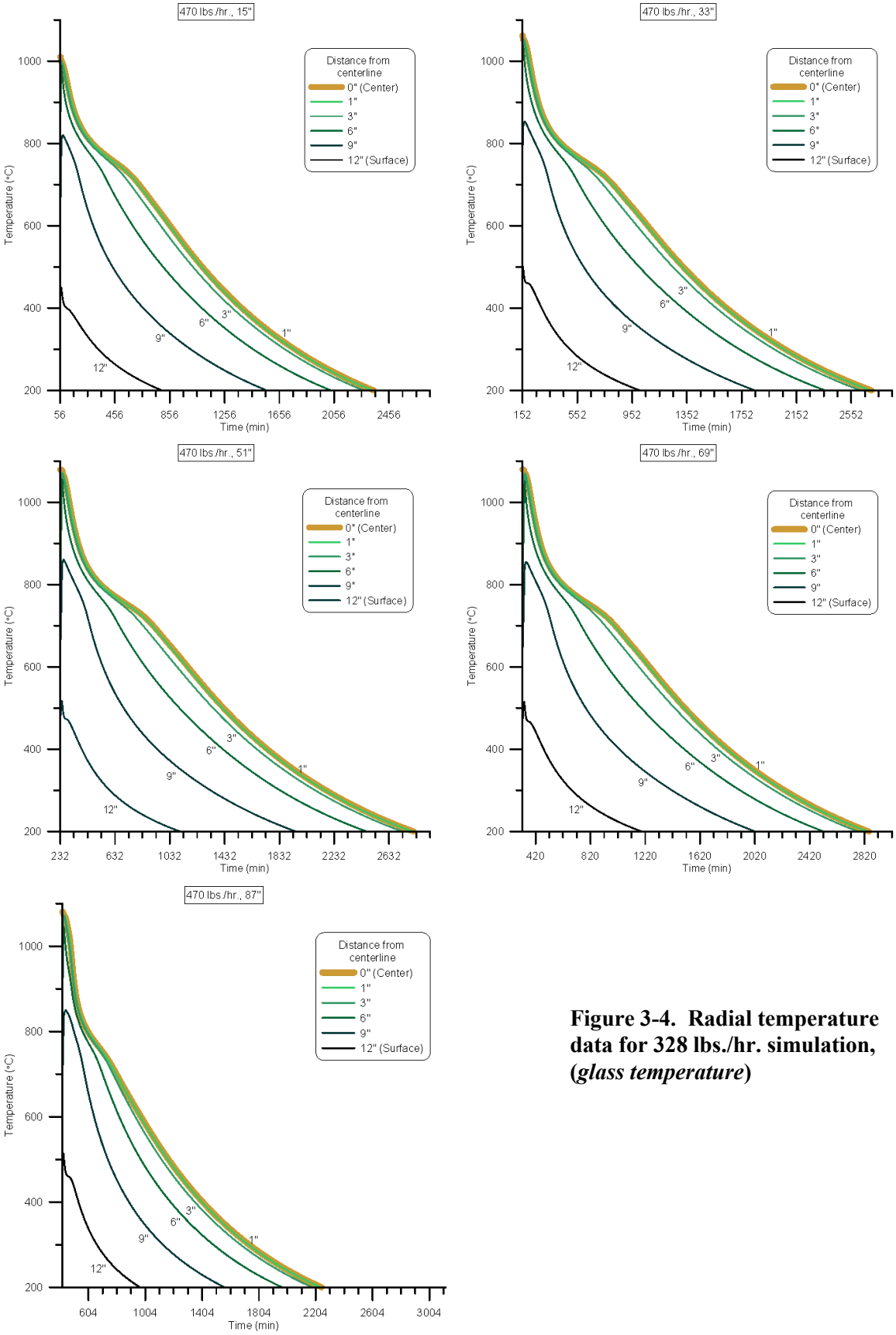

Figure 3-4. Radial temperature data for 328 lbs./hr. simulation, (*glass temperature*)

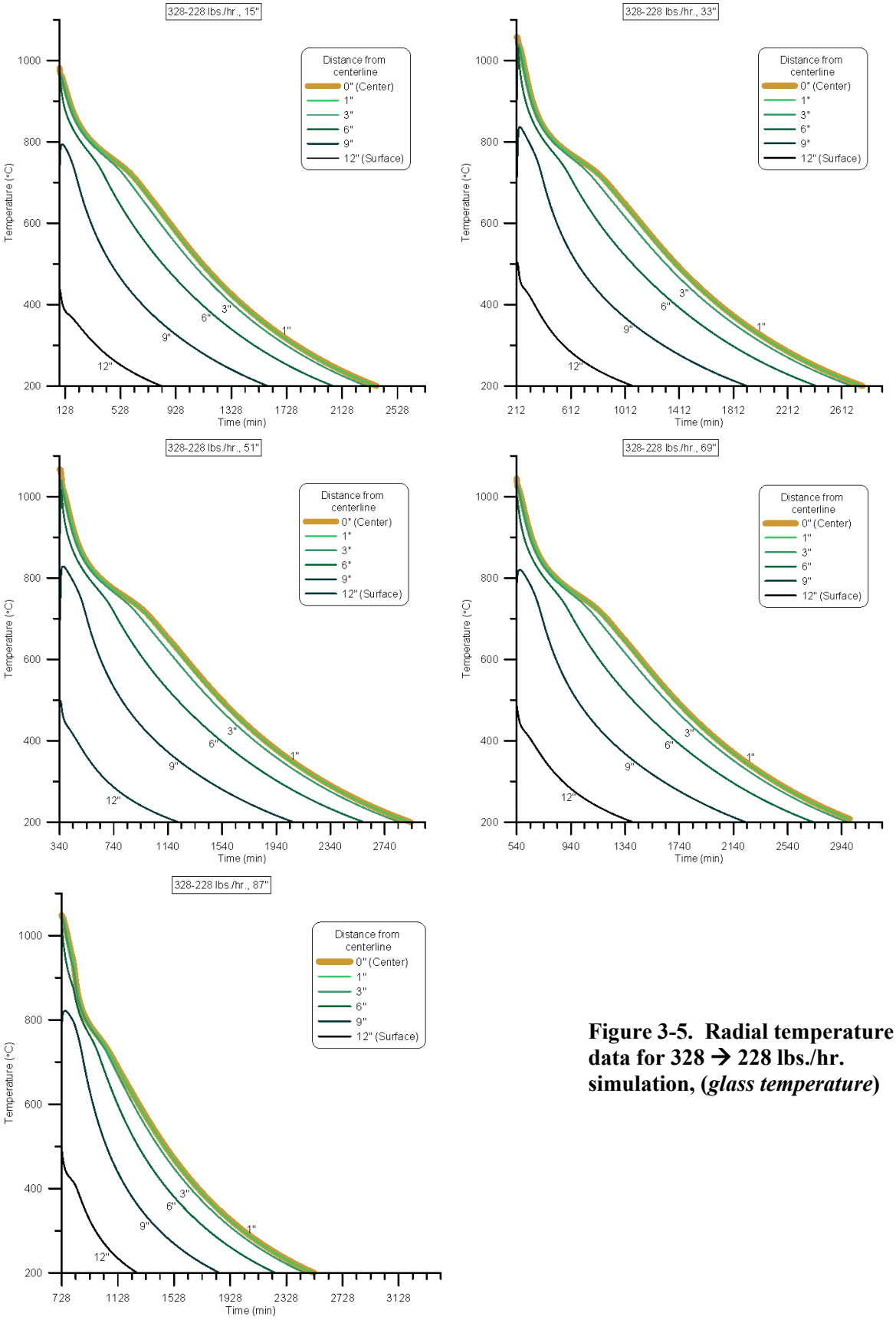

Figure 3-5. Radial temperature data for 328 → 228 lbs./hr. simulation, (*glass temperature*)

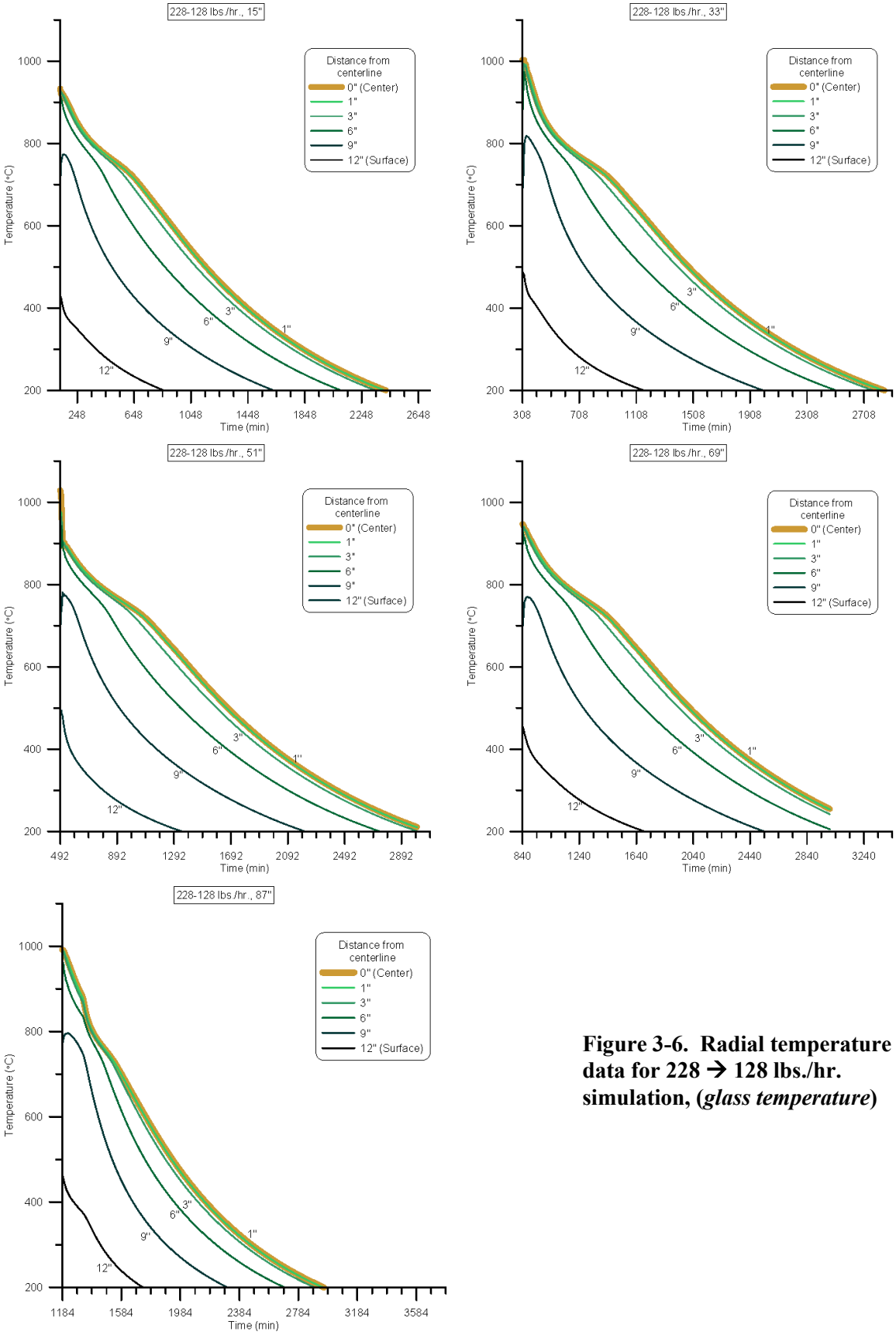

Figure 3-6. Radial temperature data for 228 → 128 lbs./hr. simulation, (*glass temperature*)

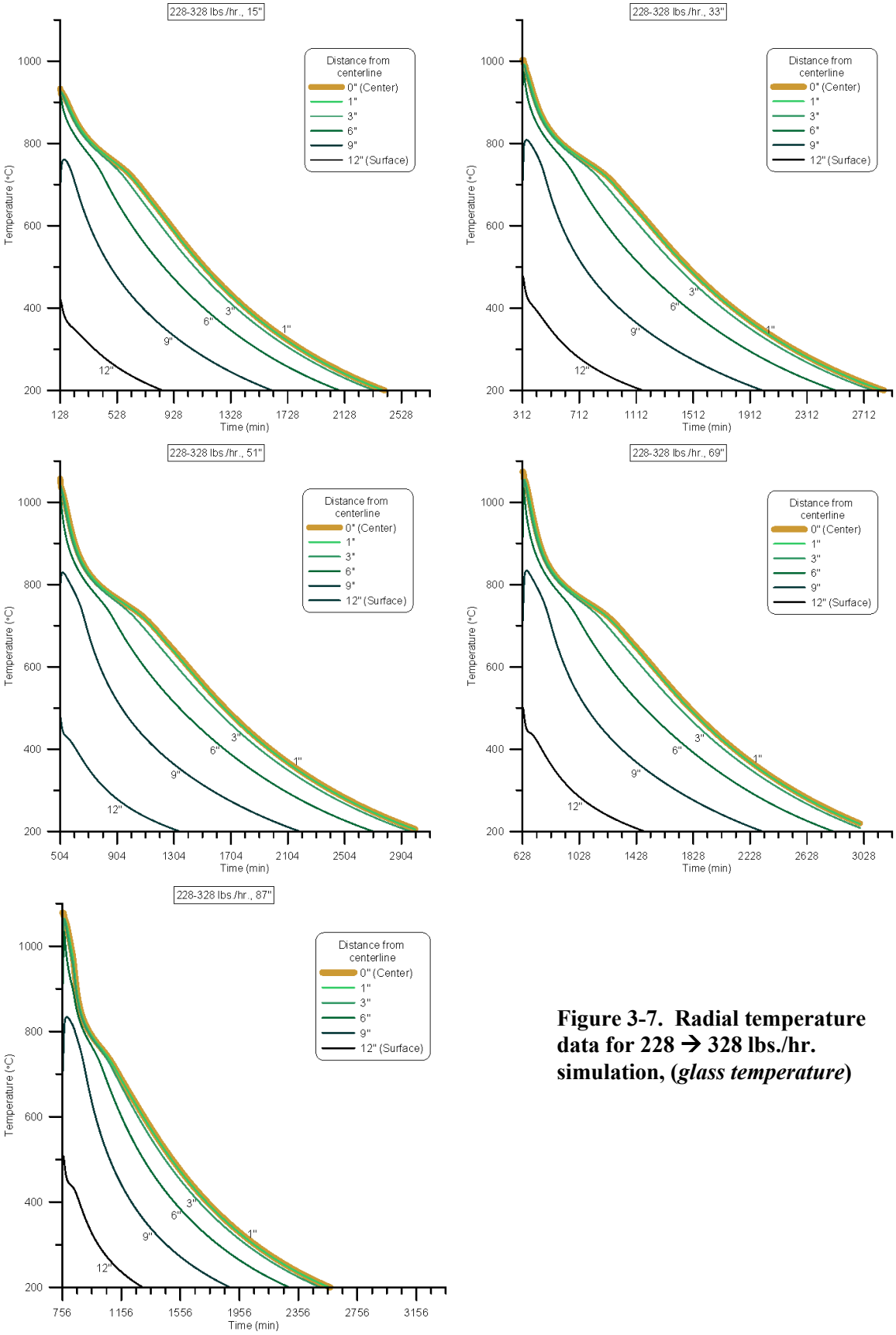

Figure 3-7. Radial temperature data for 228 → 328 lbs./hr. simulation, (*glass temperature*)

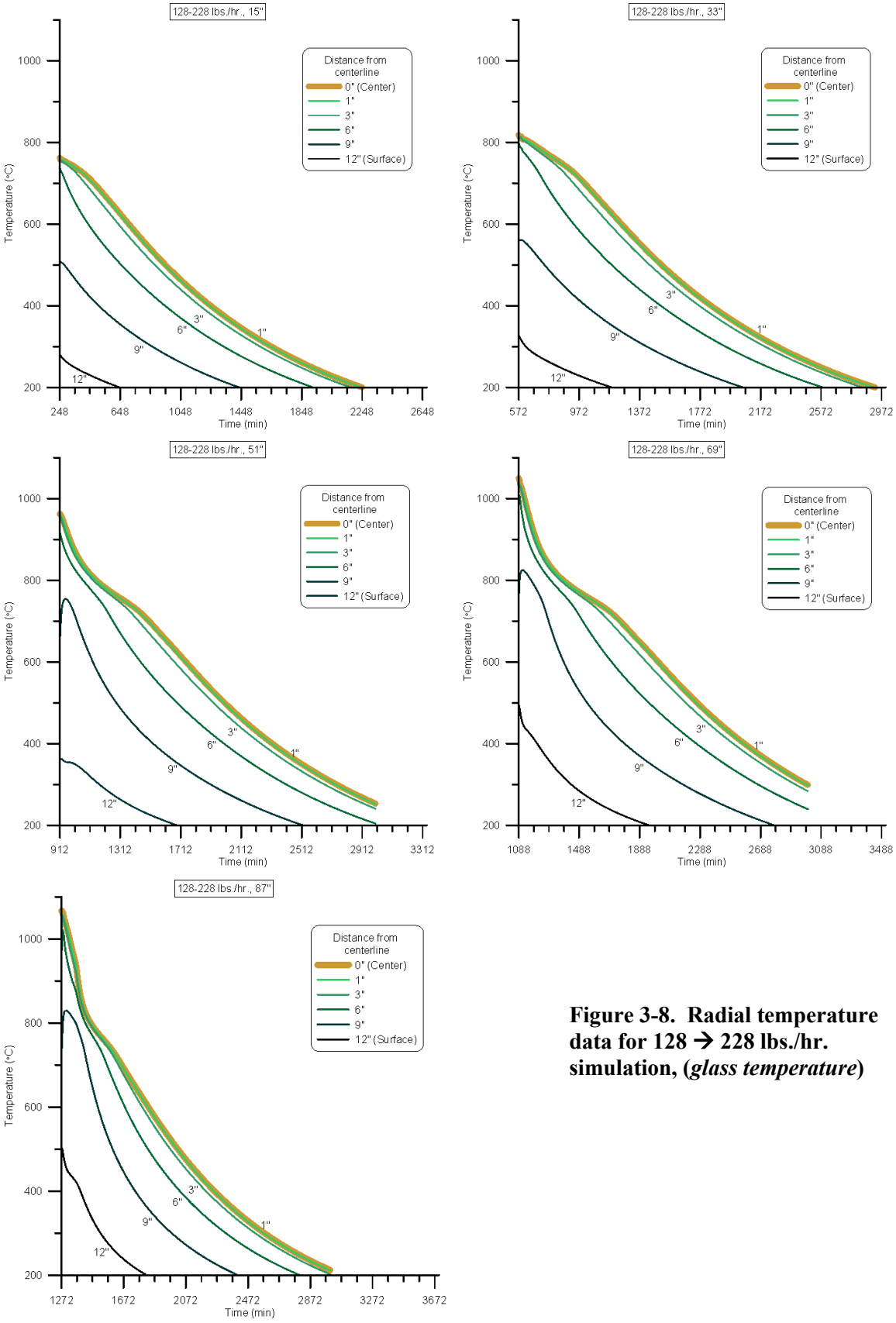

Figure 3-8. Radial temperature data for 128 → 228 lbs./hr. simulation, (*glass temperature*)

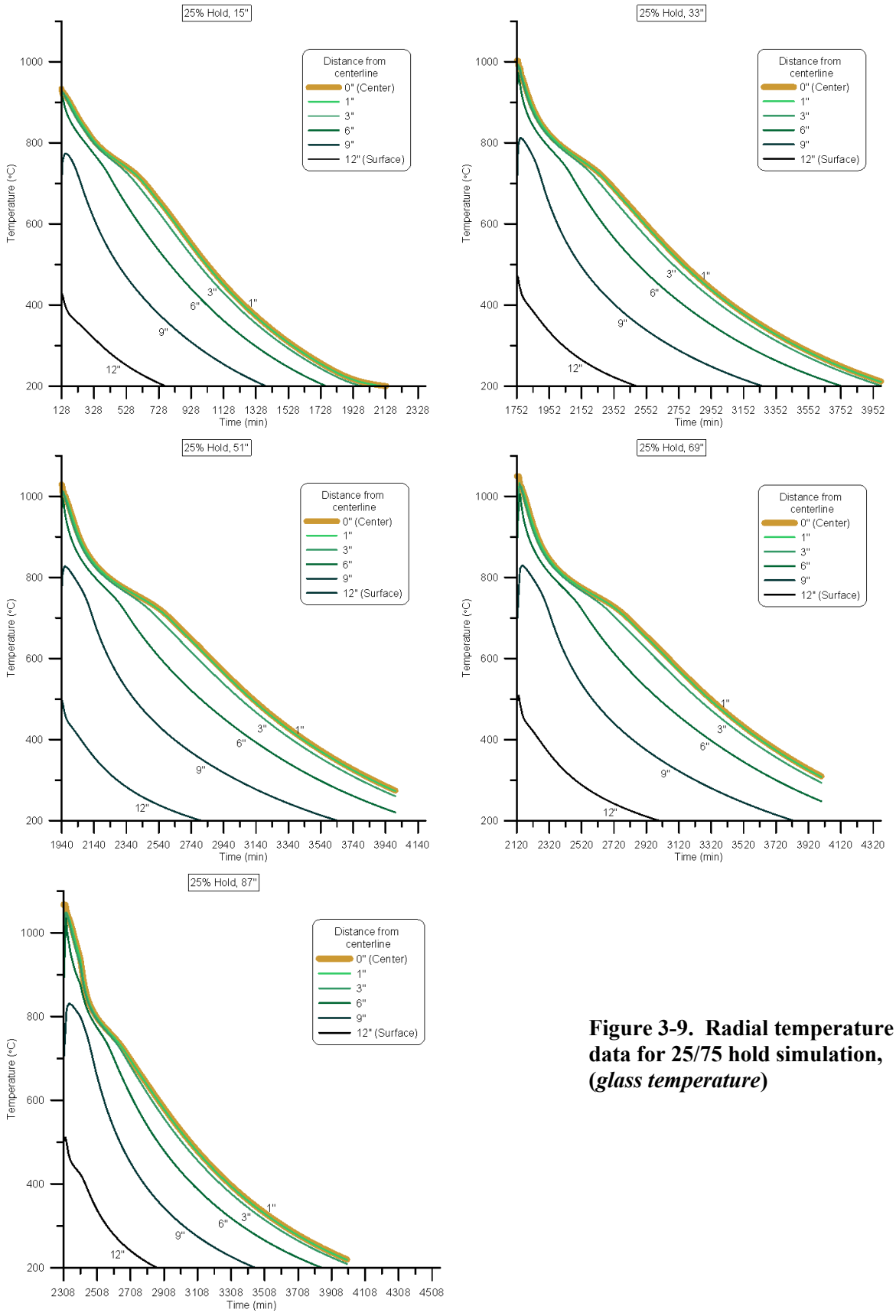

Figure 3-9. Radial temperature data for 25/75 hold simulation, (*glass temperature*)

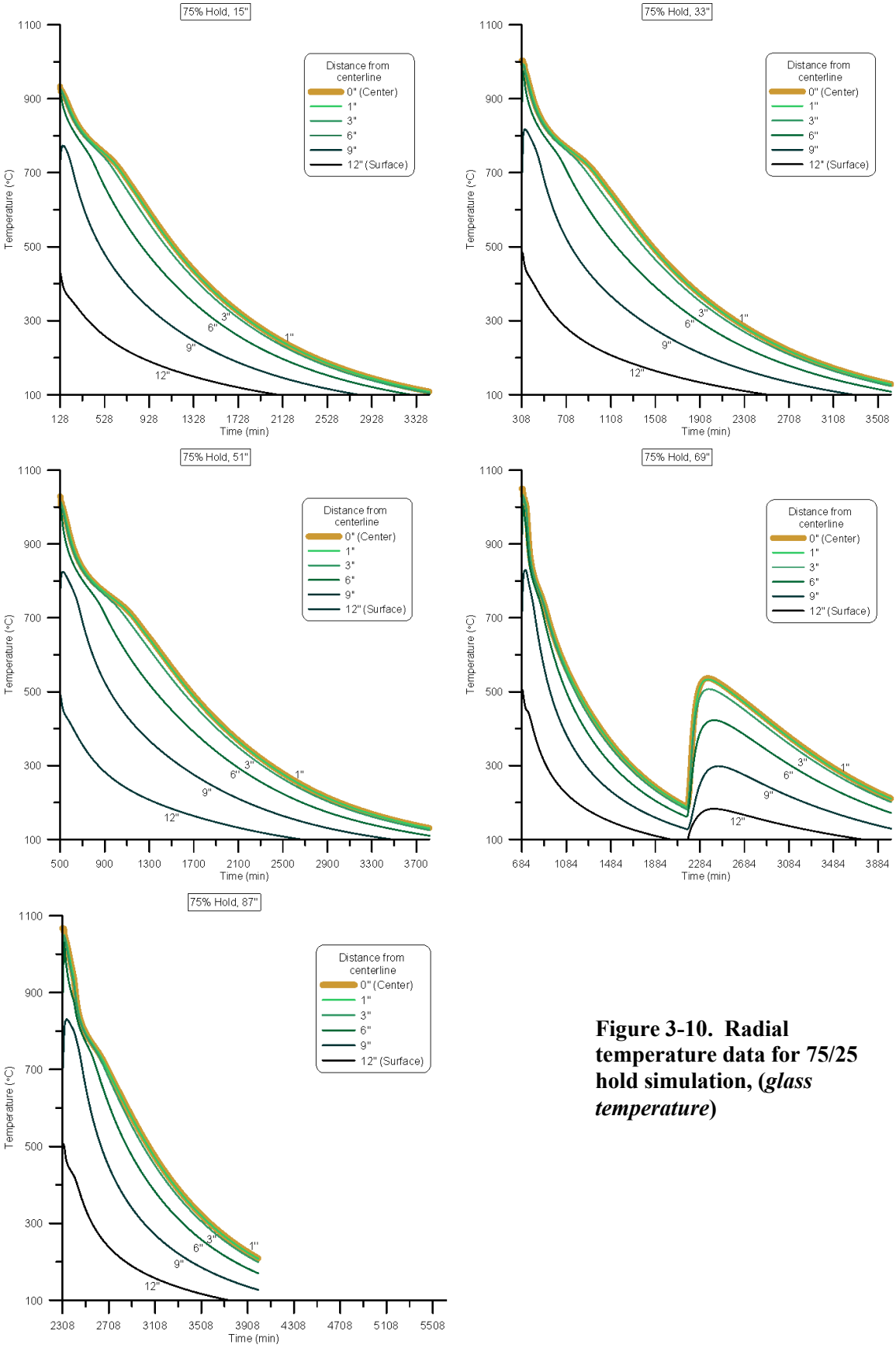

Figure 3-10. Radial temperature data for 75/25 hold simulation, (*glass temperature*)

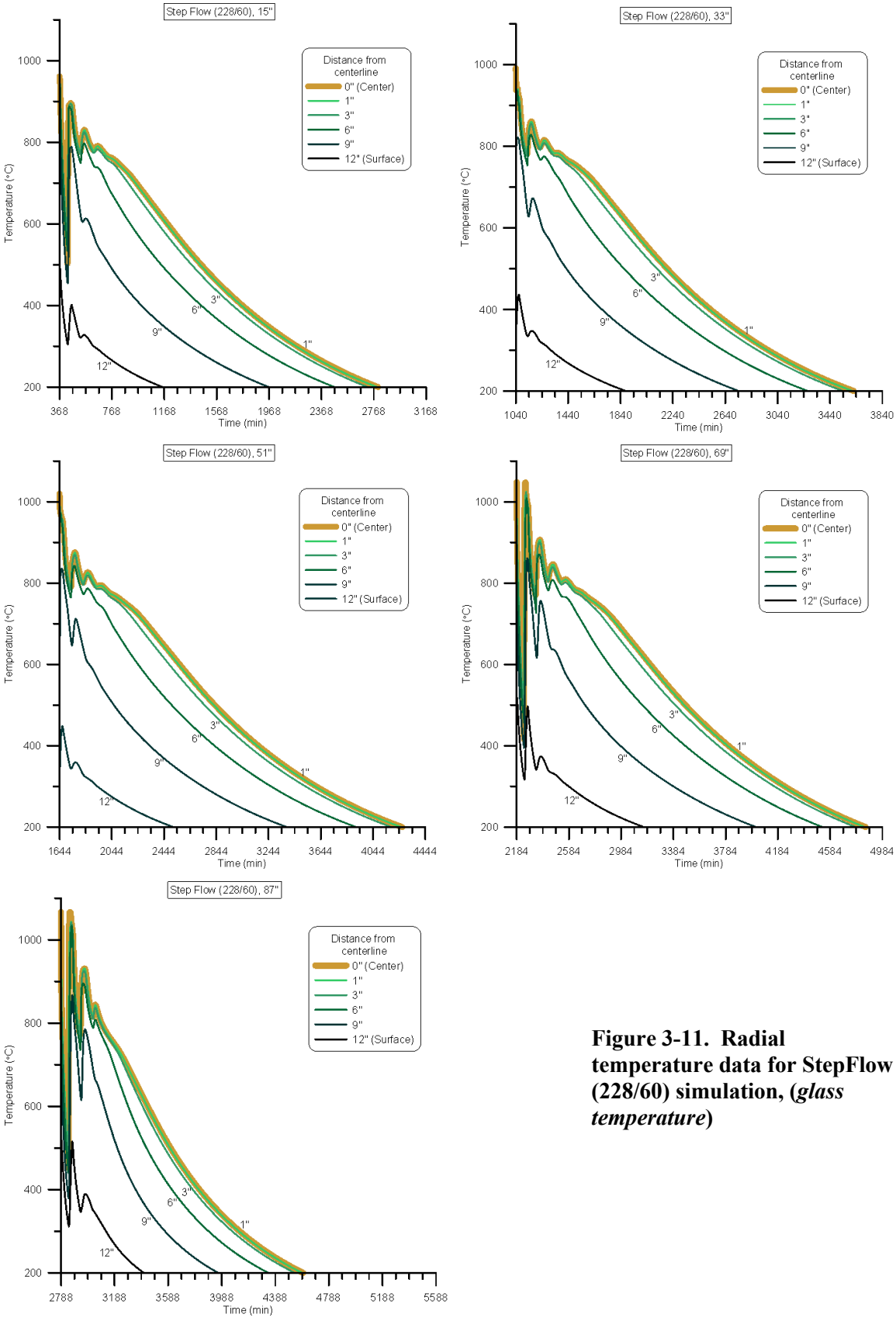

Figure 3-11. Radial temperature data for StepFlow (228/60) simulation, (*glass temperature*)

Examination of the plots in Figure 3-1 through Figure 3-11 reveals that the maximum temperature experienced by the glass, for a given height, occurs at the centerline and is reached at approximately the same time for all radial positions except the 9" radial position. The 9" radial position reaches its maximum in temperature after the maximum at the centerline (or other radial positions) has been reached. This result is consistent with the experimental data used to develop the model.[10] The source of this time lag is thought to originate from the radial heat flow from the center of the glass coupled with the heat loss to the canister wall. In effect, at the radial positions closer to the centerline (1", 3", and 6"), the heat flow from the centerline is rapid and dominates the heat loss to the canister wall, whereas at the 12" radial position the heat loss to the canister wall is rapid and dominates the heat conduction from the centerline. At the 9" radial position, heat loss to the canister wall dominates initially, but as time elapses, the heat conduction from the centerline surpasses the heat loss to the canister wall and an increase in the temperature is observed.

This time-lag effect is observed in the experimental data[10] and is a result of how the heat flow is modeled in the simulations. To aid in visualizing this effect, Figure 3-12 shows the time at which the maximum temperature is recorded as a function of radial position for the 228 lbs./hr. pour rate at the 51" height in the canister. This simulation actually indicated that the maximum time lag occurred closer to 10.5" from the centerline. This result could not be compared to experimental data as no data was found for radial distances between 9" and 12". The exact profile of this time lag is a function of the model parameters and without more experimental data to confirm the model results it is unproductive to interpret this result beyond the general trend.

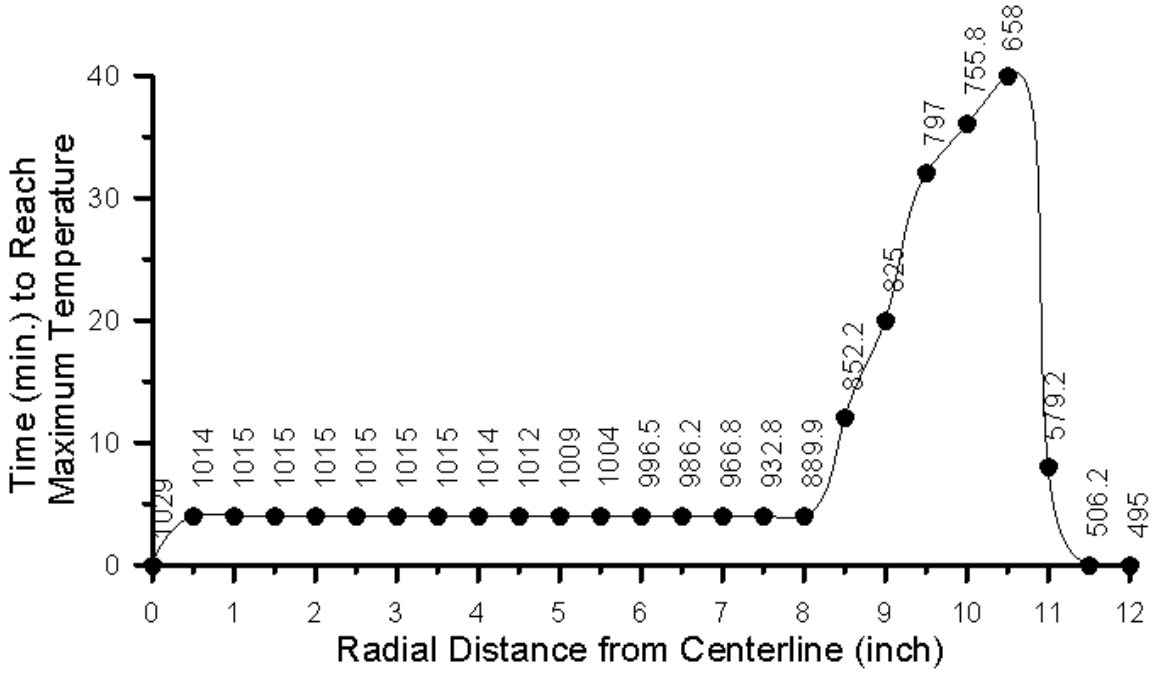

Figure 3-12. Plot showing the time lag associated with the temperature of the glass as a function of radial position. The point labels are the recorded temperatures (°C)

In order to further understand the results, the simulation radial temperature data have been plotted together according to radial position and height as shown in Figure 3-13 through Figure 3-18. Each set of simulation data was shifted along the x-axis (time) so that $x = 0$ on the plots corresponds to the maxima in temperature for the given radial position of each simulation at the specified height. Therefore, in these plots, the x-axis values represent the correct time scale but, *cannot* be related to the time during the pour simulation.[a]

The plots in Figure 3-13 through Figure 3-18 indicate that the temperature of the glass as a function of time exhibits three significant rate changes. In an attempt to semi-quantify the results, linear regression was used to fit the data in three temperature regions corresponding to the rate changes. The temperature regions chosen were T_{max}–850 °C, 850–750 °C, and 750–600 °C, where T_{max} represents the maximum temperature for a particular radial position and canister height. These temperature regions were chosen to encompass the slope changes. The fits to the data are summarized in Table 3-1, which lists the slopes, in K/min, extrapolated from each simulation.

Temperature, as a function of time, for the glass along the centerline was similar for most simulations and exhibited three distinct slope transitions. Initially, the glass cooled rapidly at ~ 0.8–1.2 K/min. from T_{max}–850 °C after which, the rate decreased to ~ 0.3 K/min. from 850–750 °C. Finally, the rate increased again to ~ 0.4 K/min. from 750–600 °C as the glass cooled similarly to conduction in a solid. As the radial distance from the centerline increased, these trends in cooling were still observed, but with diminishing similarity. In fact, at the 12" radial position, the maximum temperature recorded for any simulation did not exceed 550 °C and the cooling curves generally did not exhibit the initial changes in slope observed at the other radial positions. Rather, the cooling curves exhibited what would be expected from a rigid *solid* body in which heat flow is dominated by conduction.[b]

The significance of this result can be understood by examining the kinetics of the glass at the 12" radial distance. At the 12" radial distance, the glass would be expected to be relatively rigid since the glass transition temperature[c] (T_g) for HLW glass is typically between 450 and 480 °C. Indeed, the glass is quite rigid, as evidenced by its cooling profile in which minimal convective heat flow is observed. Therefore, the glass at the 12" radial distance can be expected to have a reduced driving force for crystallization compared to glass located closer to the centerline in which the temperature is higher comparatively. As stated previously, surface crystallization appears to dominate the nepheline crystallization observed in CCC treated samples in the laboratory.[6] Whereas the CCC simulates the cooling profile of the *glass* at 51" along the centerline of the filled canister, both the glass and crucible are heat treated together in the laboratory test. Thus, the glass/crucible interface is exposed to the same temperatures as the centerline portion of the glass in an actual canister; however, as shown in Figure 3-13 and Figure 3-18, the cooling profiles of the glass at the canister centerline and at the canister inside wall vary significantly. The simulation data suggest nepheline crystallization rates should be lower at the surface than at the centerline, whereas the CCC crucible test indicates that crystallization rates are greater at the surface than at the centerline. Based on this result, it appears that the current CCC crucible test may be conservative with respect to crystallization at the glass/canister interface.[d] The

[a] In effect, the plots in Figure 3-1 through Figure 3-11 have been overlaid and displayed on a common value time axis.
[b] For the present purposes, a solid body can be thought of as a crystalline solid (such as a metal) in which convective (kinetic) heat flow does not occur.
[c] The Tg refers to the approximate temperature that supercooled liquid converts to a solid upon cooling or vice versa. In actuality the conversion does not happen at a specific temperature (like typically assumed in crystalline materials) but rather occurs over a range of temperatures or, the glass transition range.
[d] The same can be said of the glass/air interface, though the magnitudes may not be equivalent.

simulations have demonstrated that the glass at the surface of the canister will never experience the same temperatures as the glass at the centerline and it appears that the CCC crucible test induces nepheline crystallization by increasing the kinetic (thermal) driving force for crystallization at the glass/crucible interface.

In general, the radial temperature data indicate that the pour schedule for a DWPF canister has little effect on the general trends (slopes) of the cooling curve with respect to the HLW glass. Nevertheless, adjustments to the pour schedule by way of increasing or decreasing the pour rate or intermittently pouring the glass can significantly affect the time duration at which the glass cools at a given rate. Indeed, this effect was observed to an extent in the limited pour rate data from the SGM runs.[3,12]

Table 3-1. Glass cooling rates (K/min.) for three temperature regions estimated from best-fit linear regression.

	Canister Height	15"						33"						51"						69"						87"					
	Radial Position	0"	1"	3"	6"	9"	12"	0"	1"	3"	6"	9"	12"	0"	1"	3"	6"	9"	12"	0"	1"	3"	6"	9"	12"	0"	1"	3"	6"	9"	12"
T_{max}-850 °C	119 lbs./hr.	-	-	-	-	-	-	-	-	-	-	-	-	-	-	-	-	-	-	-0.6	-0.6	-0.7	-1.0	-	-	-0.8	-0.8	-0.9	-0.9	-	-
	228 lbs./hr.	-0.7	-0.7	-0.8	-1.2	-	-	-1.0	-0.9	-1.1	-1.3	-	-	-1.1	-1.0	-1.1	-1.3	-	-	-1.1	-1.1	-1.2	-1.3	-	-	-1.6	-1.6	-1.7	-1.6	-	-
	328 lbs./hr.	-1.0	-1.0	-1.0	-1.4	-	-	-1.2	-1.2	-1.3	-1.5	-	-	-1.3	-1.3	-1.3	-1.4	-	-	-1.3	-1.3	-1.4	-1.5	-	-	-2.0	-2.2	-2.1	-2.0	-	-
	470 lbs./hr.	-1.3	-1.3	-1.4	-1.7	-	-	-1.3	-1.4	-1.4	-1.5	-	-	-1.4	-1.4	-1.5	-1.6	-	-	-1.4	-1.4	-1.5	-1.5	-	-	-2.2	-2.4	-2.4	-2.4	-	-
	328-228 lbs./hr.	-1.0	-1.0	-1.1	-1.5	-	-	-1.3	-1.3	-1.3	-1.5	-	-	-1.2	-1.1	-1.2	-1.4	-	-	-1.1	-1.1	-1.2	-1.3	-	-	-1.6	-1.7	-1.7	-1.6	-	-
	228-128 lbs./hr.	-0.7	-0.7	-0.8	-1.2	-	-	-1.0	-1.0	-1.1	-1.3	-	-	-0.9	-0.7	-0.7	-1.5	-	-	-0.6	-0.6	-0.7	-1.0	-	-	-0.9	-0.9	-0.9	-1.0	-	-
	228-328 lbs./hr.	-0.7	-0.7	-0.8	-1.3	-	-	-1.0	-1.0	-1.1	-1.3	-	-	-1.3	-1.3	-1.3	-1.7	-	-	-1.4	-1.3	-1.4	-1.5	-	-	-2.0	-2.1	-2.2	-2.0	-	-
	128-228 lbs./hr.	-	-	-	-	-	-	-	-	-	-	-	-	-0.9	-0.9	-1.0	-1.1	-	-	-1.2	-1.1	-1.2	-1.3	-	-	-1.7	-1.7	-1.7	-1.6	-	-
	228 lbs./hr.; 25/75 Hold	-0.7	-0.7	-0.8	-1.2	-	-	-1.1	-1.1	-1.1	-1.5	-	-	-1.1	-1.0	-1.1	-1.3	-	-	-1.1	-1.1	-1.2	-1.3	-	-	-1.6	-1.7	-1.7	-1.6	-	-
	228 lbs./hr.; 75/25 Hold	-0.7	-0.7	-0.8	-1.2	-	-	-1.0	-1.0	-1.0	-1.3	-	-	-1.1	-1.0	-1.1	-1.3	-	-	-2.6	-2.8	-2.9	-3.0	-	-	-1.6	-1.7	-1.7	-1.6	-	-
	StepFlow: (228/60)	-	-	-	-	-	-	-	-	-	-	-	-	-	-	-	-	-	-	-	-	-	-	-	-	-	-	-		-	-
	Canister Height	15"						33"						51"						69"						87"					
	Radial Position	0"	1"	3"	6"	9"	12"	0"	1"	3"	6"	9"	12"	0"	1"	3"	6"	9"	12"	0"	1"	3"	6"	9"	12"	0"	1"	3"	6"	9"	12"
850-750°C	119 lbs./hr.	-	-	-	-	-	-	-	-	-	-	-	-	-0.3	-	-0.3	-0.5	-	-	-0.3	-0.3	-0.3	-0.4	-	-	-0.6	-0.6	-0.7	-0.6	-	-
	228 lbs./hr.	-0.3	-0.3	-0.4	-0.5	-0.5	-	-0.3	-0.3	-0.3	-0.4	-0.6	-	-0.3	-0.3	-0.3	-0.5	-0.6	-	-0.3	-0.3	-0.3	-0.4	-0.6	-	-0.6	-0.6	-0.6	-0.8	-0.8	-
	328 lbs./hr.	-0.3	-0.3	-0.4	-0.5	-0.7	-	-0.3	-0.3	-0.3	-0.5	-0.7	-	-0.3	-0.3	-0.3	-0.5	-0.7	-	-0.3	-0.3	-0.3	-0.5	-0.7	-	-0.6	-0.6	-0.6	-0.7	-0.9	-
	470 lbs./hr.	-0.3	-0.3	-0.4	-0.5	-0.8	-	-0.3	-0.3	-0.3	-0.5	-0.7	-	-0.3	-0.3	-0.3	-0.5	-0.7	-	-0.3	-0.3	-0.3	-0.5	-0.7	-	-0.5	-0.5	-0.6	-0.7	-1.0	-
	328-228 lbs./hr.	-0.3	-0.3	-0.4	-0.5	-0.6	-	-0.3	-0.3	-0.3	-0.5	-0.6	-	-0.3	-0.3	-0.3	-0.5	-0.6	-	-0.3	-0.3	-0.3	-0.5	-0.6	-	-0.6	-0.6	-0.6	-0.8	-0.7	-
	228-128 lbs./hr.	-0.3	-0.3	-0.4	-0.5	-0.5	-	-0.3	-0.3	-0.3	-0.4	-0.6	-	-0.3	-0.3	-0.3	-0.4	-0.7	-	-0.3	-0.3	-0.3	-0.4	-0.4	-	-0.6	-0.6	-0.6	-0.8	-0.5	-
	228-328 lbs./hr.	-0.3	-0.3	-0.4	-0.5	-0.4	-	-0.3	-0.3	-0.3	-0.4	-0.6	-	-0.3	-0.3	-0.3	-0.5	-	-	-0.3	-0.3	-0.3	-0.5	-0.7	-	-0.6	-0.6	-0.6	-0.7	-0.9	-
	128-228 lbs./hr.	-0.2	-0.2	-0.2	-	-	-	-	-0.2	-0.2	-0.5	-	-	-	-0.3	-0.4	-0.5	-	-	-0.3	-0.3	-0.3	-0.4	-0.6	-	-0.6	-0.6	-0.6	-0.8	-0.8	-
	228 lbs./hr.; 25/75 Hold	-0.4	-0.4	-0.4	-0.5	-0.5	-	-0.3	-0.3	-0.4	-0.5	-0.7	-	-0.3	-0.3	-0.3	-0.4	-0.6	-	-0.3	-0.3	-0.3	-0.4	-0.6	-	-0.6	-0.6	-0.6	-0.8	-0.7	-
	228 lbs./hr.; 75/25 Hold	-0.3	-0.3	-0.4	-0.5	-0.5	-	-0.3	-0.3	-0.3	-0.4	-0.6	-	-0.3	-0.3	-0.3	-0.4	-0.6	-	-0.9	-0.9	-0.9	-1.0	-1.4	-	-0.6	-0.6	-0.6	-0.8	-0.7	-
	StepFlow: (228/60)	-	-	-	-	-	-	-	-	-	-	-	-	-	-	-	-	-	-	-	-	-	-	-	-	-	-	-	-	-	-
	Canister Height	15"						33"						51"						69"						87"					
	Radial Position	0"	1"	3"	6"	9"	12"	0"	1"	3"	6"	9"	12"	0"	1"	3"	6"	9"	12"	0"	1"	3"	6"	9"	12"	0"	1"	3"	6"	9"	12"
750-600 °C	119 lbs./hr.	-0.4	-0.4	-0.5	-0.9	-	-	-0.4	-0.4	-0.4	-0.6	-	-	-0.4	-0.4	-0.4	-0.6	-	-	-0.4	-0.4	-0.4	-0.6	-	-	-0.6	-0.6	-0.7	-0.9	-0.7	-
	228 lbs./hr.	-0.4	-0.4	-0.4	-0.6	-1.1	-	-0.4	-0.4	-0.4	-0.6	-1.1	-	-0.4	-0.4	-0.4	-0.6	-1.0	-	-0.4	-0.4	-0.4	-0.6	-1.1	-	-0.6	-0.6	-0.7	-0.9	-1.6	-
	328 lbs./hr.	-0.4	-0.4	-0.4	-0.6	-1.1	-	-0.4	-0.4	-0.4	-0.6	-1.1	-	-0.4	-0.4	-0.4	-0.6	-1.0	-	-0.4	-0.4	-0.4	-0.6	-1.1	-	-0.6	-0.6	-0.7	-0.9	-1.6	-
	470 lbs./hr.	-0.4	-0.4	-0.4	-0.6	-1.2	-	-0.4	-0.4	-0.4	-0.6	-1.1	-	-0.4	-0.4	-0.4	-0.6	-1.0	-	-0.4	-0.4	-0.4	-0.6	-1.1	-	-0.5	-0.6	-0.7	-0.9	-1.6	-
	328-228 lbs./hr.	-0.4	-0.4	-0.4	-0.6	-1.1	-	-0.4	-0.4	-0.4	-0.6	-1.1	-	-0.4	-0.4	-0.4	-0.6	-1.0	-	-0.4	-0.4	-0.4	-0.6	-1.1	-	-0.6	-0.6	-0.7	-0.9	-1.6	-
	228-128 lbs./hr.	-0.4	-0.4	-0.4	-0.6	-1.1	-	-0.4	-0.4	-0.4	-0.6	-1.1	-	-0.4	-0.4	-0.4	-0.6	-1.0	-	-0.4	-0.4	-0.4	-0.6	-0.9	-	-0.6	-0.6	-0.7	-0.9	-1.5	-
	228-328 lbs./hr.	-0.4	-0.4	-0.4	-0.6	-1.0	-	-0.4	-0.4	-0.4	-0.6	-1.1	-	-0.4	-0.4	-0.4	-0.6	-1.0	-	-0.4	-0.4	-0.4	-0.6	-1.1	-	-0.6	-0.6	-0.7	-0.9	-1.6	-
	128-228 lbs./hr.	-0.4	-0.4	-0.4	-0.7	-	-	-0.4	-0.4	-0.4	-0.6	-	-	-0.4	-0.4	-0.4	-0.6	-1.0	-	-0.4	-0.4	-0.4	-0.6	-1.1	-	-0.6	-0.6	-0.7	-0.9	-1.6	-
	228 lbs./hr.; 25/75 Hold	-0.4	-0.5	-0.5	-0.6	-1.1	-	-0.4	-0.4	-0.4	-0.6	-1.2	-	-0.4	-0.4	-0.4	-0.6	-1.0	-	-0.4	-0.4	-0.4	-0.6	-1.1	-	-0.6	-0.6	-0.7	-0.9	-1.6	-
	228 lbs./hr.; 75/25 Hold	-0.4	-0.4	-0.4	-0.6	-1.1	-	-0.4	-0.4	-0.4	-0.6	-1.1	-	-0.4	-0.4	-0.4	-0.6	-1.0	-	-1.0	-1.0	-1.0	-1.2	-1.7	-	-0.6	-0.6	-0.7	-0.9	-1.6	-
	StepFlow: (228/60)	-	-	-	-	-	-	-	-	-	-	-	-	-0.4	-0.4	-0.4	-0.6	-	-	-0.4	-0.4	-0.4	-0.6	-	-	-	-	-0.7	-0.9	-	-

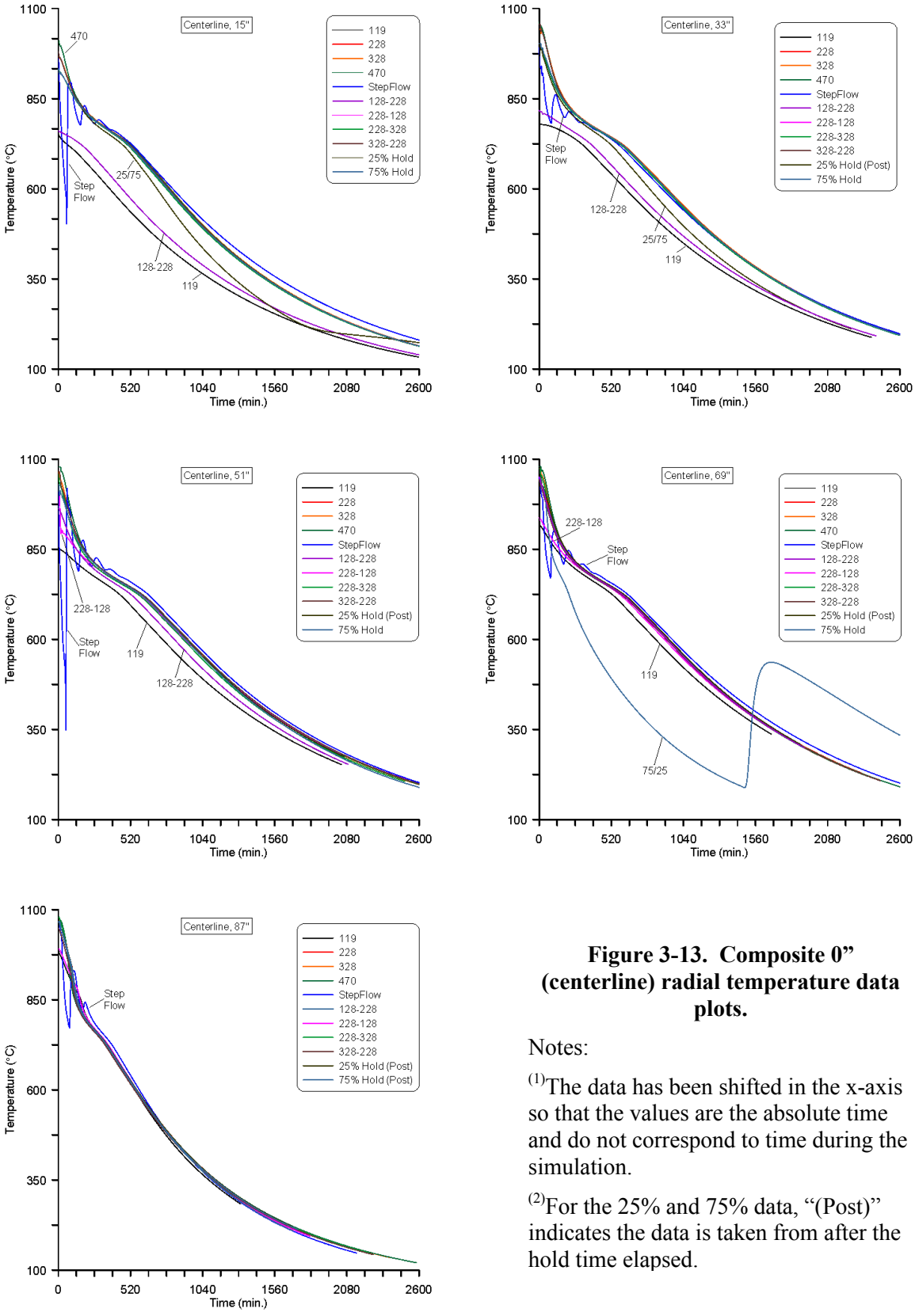

Figure 3-13. Composite 0" (centerline) radial temperature data plots.

Notes:

(1)The data has been shifted in the x-axis so that the values are the absolute time and do not correspond to time during the simulation.

(2)For the 25% and 75% data, "(Post)" indicates the data is taken from after the hold time elapsed.

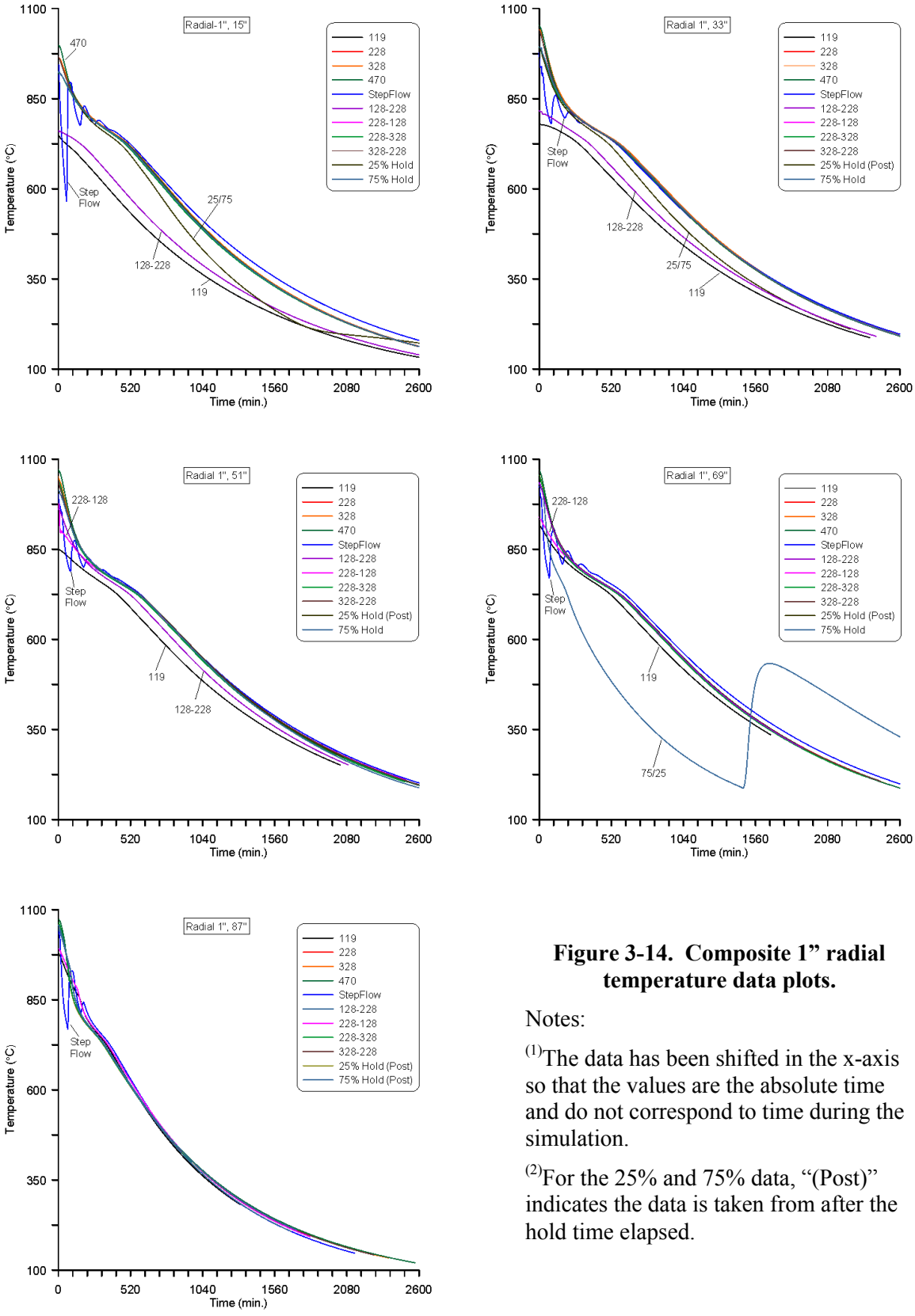

Figure 3-14. Composite 1" radial temperature data plots.

Notes:

(1)The data has been shifted in the x-axis so that the values are the absolute time and do not correspond to time during the simulation.

(2)For the 25% and 75% data, "(Post)" indicates the data is taken from after the hold time elapsed.

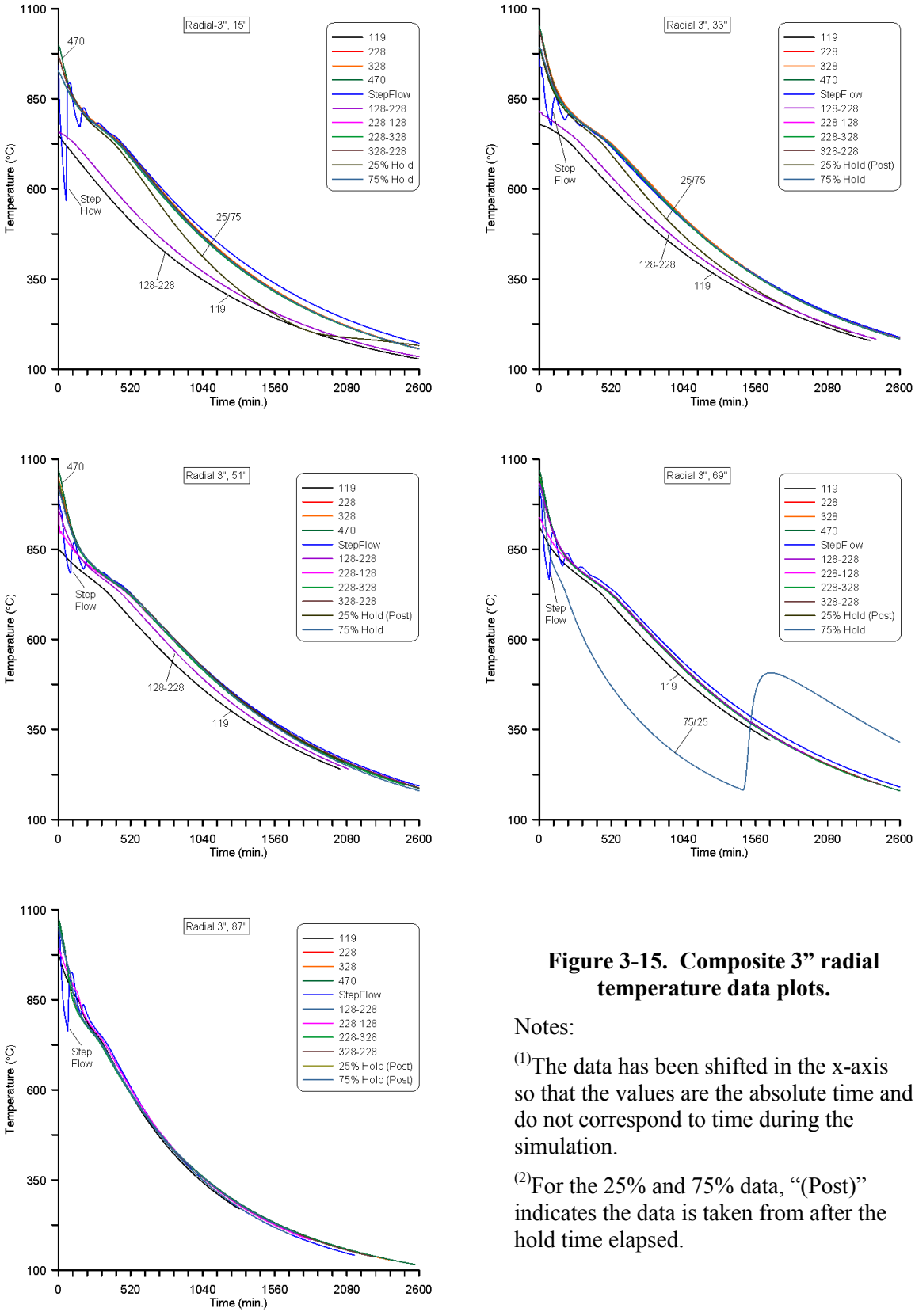

Figure 3-15. Composite 3" radial temperature data plots.

Notes:

(1)The data has been shifted in the x-axis so that the values are the absolute time and do not correspond to time during the simulation.

(2)For the 25% and 75% data, "(Post)" indicates the data is taken from after the hold time elapsed.

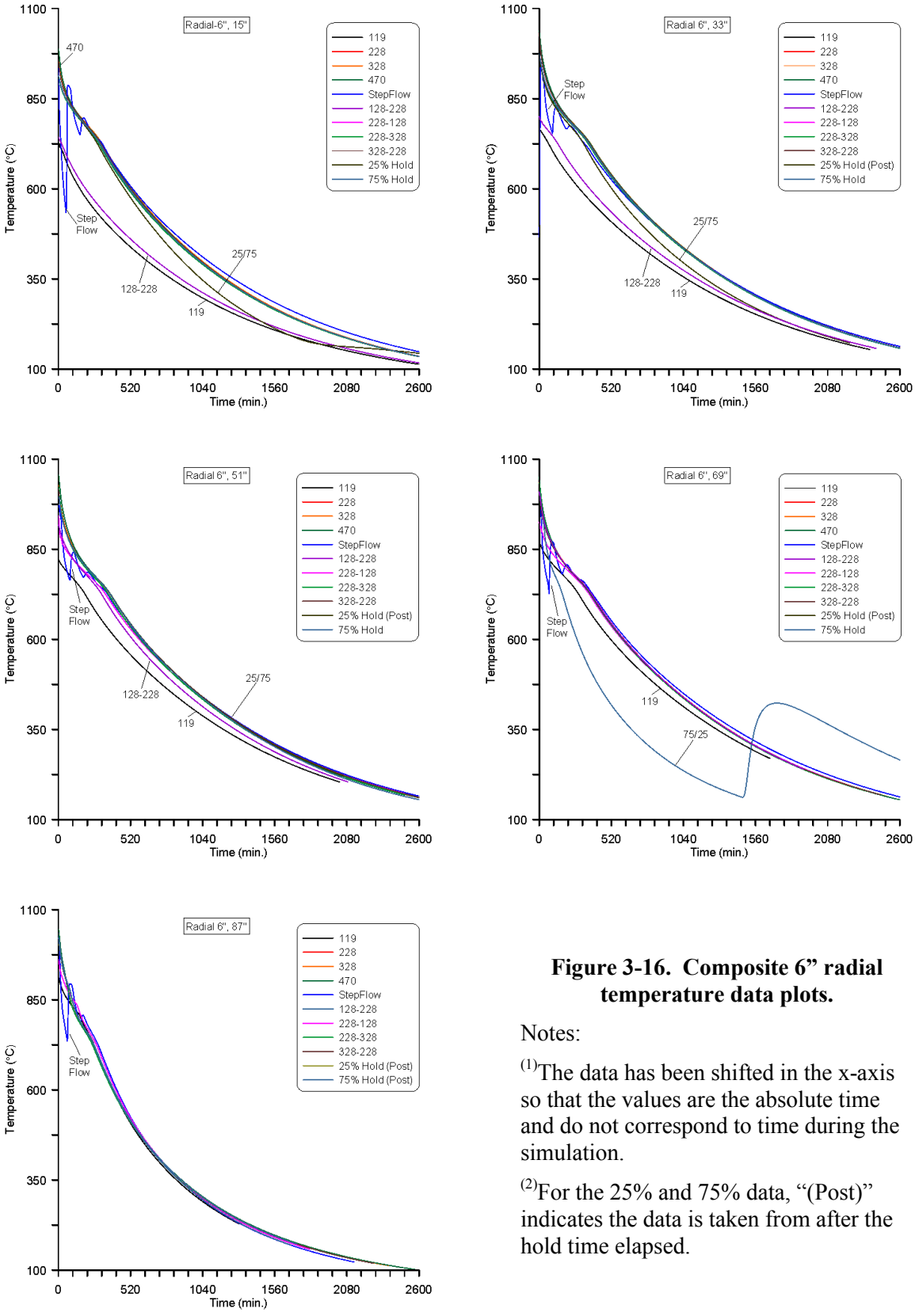

Figure 3-16. Composite 6" radial temperature data plots.

Notes:

(1)The data has been shifted in the x-axis so that the values are the absolute time and do not correspond to time during the simulation.

(2)For the 25% and 75% data, "(Post)" indicates the data is taken from after the hold time elapsed.

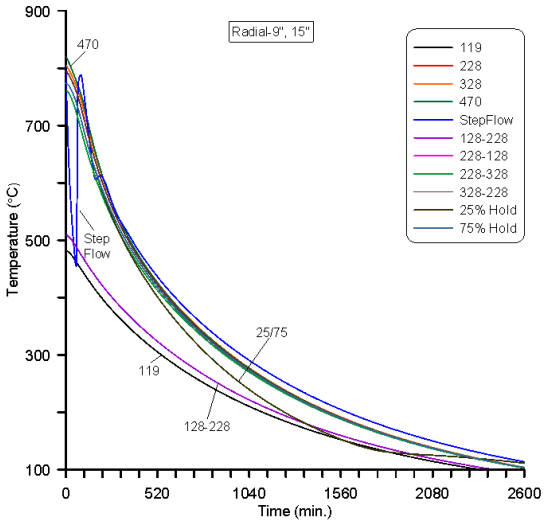

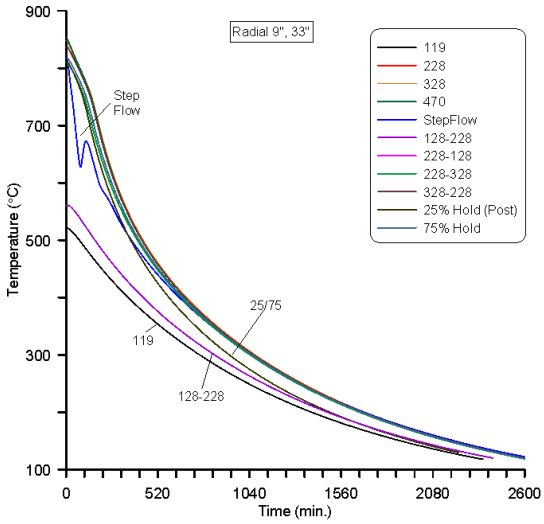

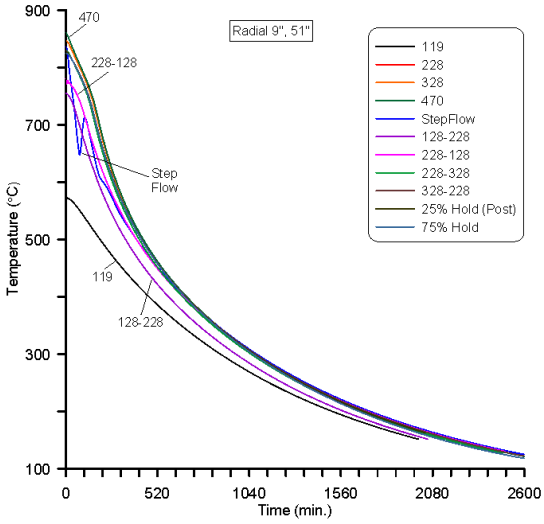

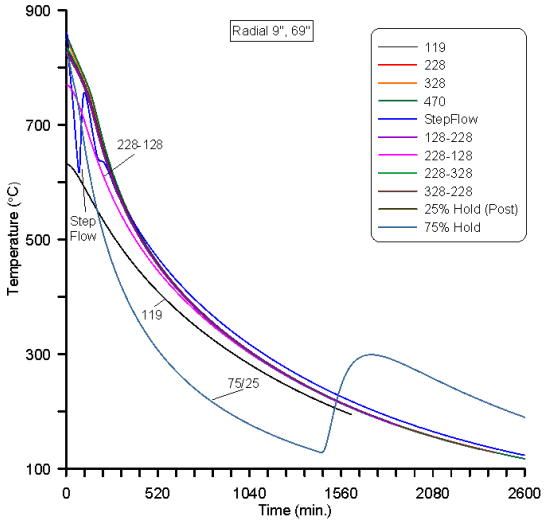

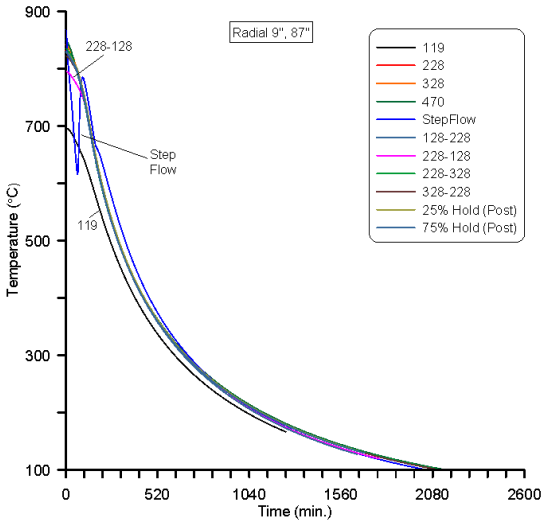

Figure 3-17. Composite 9" radial temperature data plots.

Notes:

[1]The data has been shifted in the x-axis so that the values are the absolute time and do not correspond to time during the simulation.

[2]For the 25% and 75% data, "(Post)" indicates the data is taken from after the hold time elapsed.

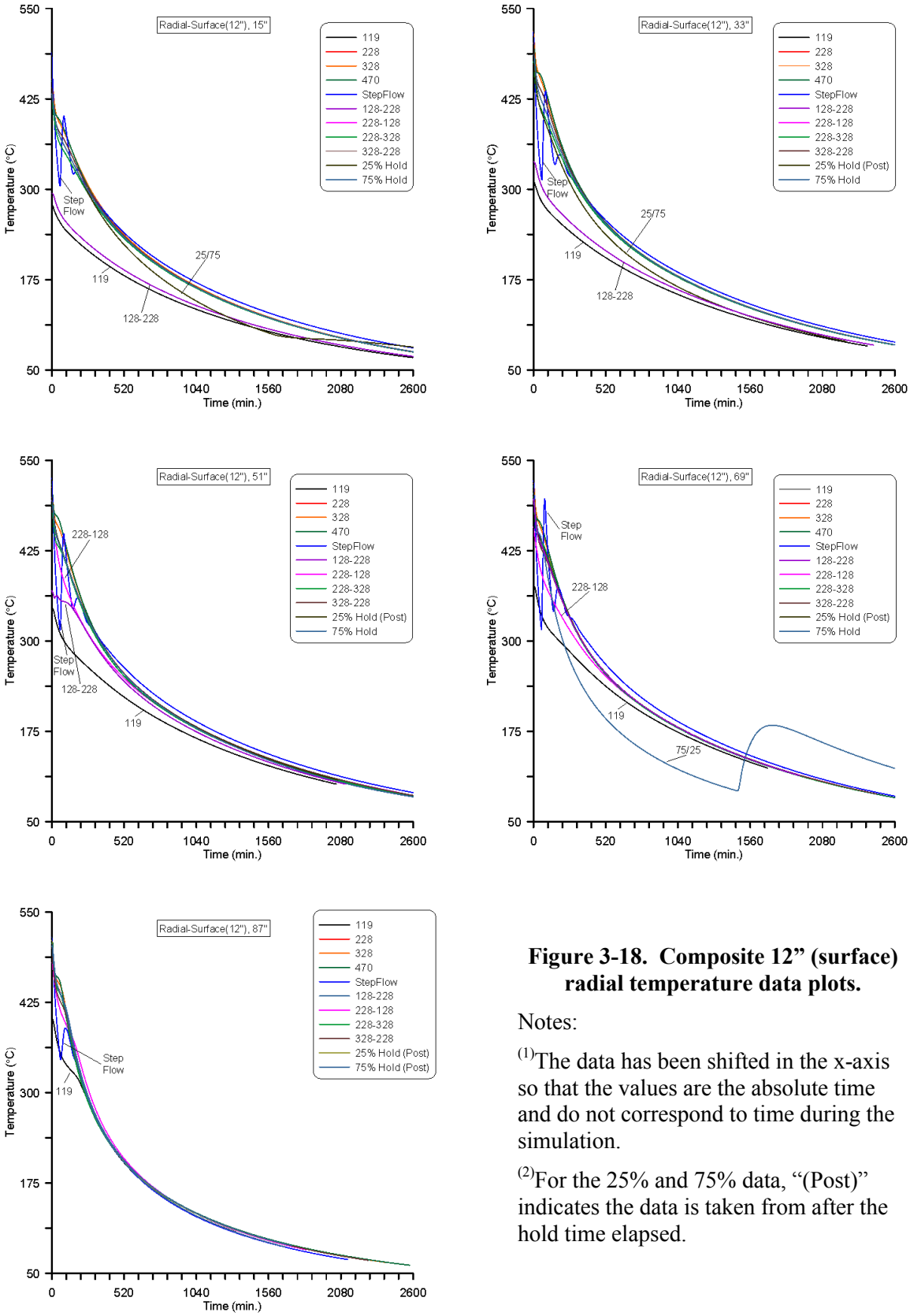

Figure 3-18. Composite 12" (surface) radial temperature data plots.

Notes:

(1)The data has been shifted in the x-axis so that the values are the absolute time and do not correspond to time during the simulation.

(2)For the 25% and 75% data, "(Post)" indicates the data is taken from after the hold time elapsed.

3.2 Temperature Dwell Charts

Another goal of this research was to identify areas within a HLW glass filled canister that may be at increased probability of crystallization due to kinetic effects. Assuming that nepheline crystallization increases with the time that the glass remains at nucleation and growth temperatures, temperature dwell charts are useful in identifying such crystallization prone areas within a HLW glass filled canister. The temperature dwell charts generated from the simulations are shown in Figure 3-19 through Figure 3-29. As described previously, the temperature dwell charts contain temperature data about the entire volume of the glass. The radial temperature data discussed beforehand (Section 3.1) are embedded in the temperature dwell charts even if not clearly apparent to the eye. As such, this discussion will focus on the additional and complementary information provided by these charts compared to the radial temperature data. In interpreting the temperature dwell charts it is critical to recall that the time duration of the pour is compressed (lost) in these charts; instead, they represent the total elapsed time any portion of the glass remained within the specified temperature range.

Table 3-2 summarizes the maximum temperature dwell time results. For all simulations, on average, portions of the glass spent nearly 400 minutes within the 700 °C–800 °C temperature range, the longest time of any of the experimental temperature regions. Portions of the glass remained for the least amount of time within the 1100 °C–900 °C temperature range and, on average the glass remained above 1000 °C for 30% of that time. In most simulations, the glass remained between 700 °C–600 °C or for a longer period of time than between 900 °C–800 °C. These results are consistent with the cooling profiles described earlier in which multiple rate changes are observed during the total cooling time. In the study simulations, the time that any portion of the glass remained within 600 °C–700 °C, 700 °C–800 °C, 800 °C–900 °C, 900 °C–1000 °C, or 1000 °C–1100 °C could be changed by 71, 94, 134, 60, or 45 minutes respectively by adjusting the pour rate. These results suggest that the pour rate can significantly impact the resultant temperatures and time that portions of HLW glass in DWPF canisters might be exposed to and it is important to understand the impact that changes to the pour rate have on the tendency to form nepheline.

Table 3-2. Summary of time-temperature dwell data from simulations.

Simulation	Time (minutes)				
	600-700 °C	700-800 °C	800-900 °C	900-1000 °C	1000-1100 °C
119 lbs./hr.	325.0	403.3	227.4	101.1	11.9
228 lbs./hr.	254.2	378.4	203.4	101.0	48.6
328 lbs./hr.	254.1	381.2	172.2	93.7	52.5
470 lbs./hr.	255.3	383.6	167.5	79.6	56.7
328-228 lbs./hr.	254.8	381.6	180.5	89.8	46.5
228-128 lbs./hr.	258.5	388.4	260.1	120.9	26.2
228-328 lbs./hr.	257.2	381.5	198.4	95.7	49.7
128-228 lbs./hr.	256.9	407.1	265.3	84.3	48.0
228 lbs./hr.; 25/75 Hold	304	378.5	201.8	99.3	48.5
228 lbs./hr.; 75/25 Hold	317.7	378.0	203.4	101.0	48.6
StepFlow: (228/60)	277	472.3	301.1	60.5	23.8

Although the maximum dwell times shown in Table 3-2 indicate extremes, they alone do not indicate the total volume or, location within the canister of the glass at said temperature. Non-uniform temperatures within the canister could result in non-uniform crystallization. In general, 'hot spots' (areas of the glass that remained at an elevated temperature relative to their immediate surroundings) and radial or vertical temperature gradients (as a function of dwell time) within the canister will contribute to non-uniform dwell times of the glass within the canister. Note that color gradients in the charts represent a gradient in time (again, the time duration is compressed) within the specified temperature region.

Hot spots between 900–1000 °C were observed approximately 13" from the canister bottom in the 470 lbs./hr. simulation and approximately 18" from the canister bottom in the 328 lbs./hr. and 328→228 lbs./hr. simulations. Hot spots were observed between 900–1000 °C approximately 42" from the canister bottom in the 228 lbs./hr., 75/25, 25/75, and step flow (228/60) simulations. Hot spots were also observed at approximately 10" between 800–900 °C in the 228 lbs./hr., 228→128 lbs./hr., 228→328 lbs./hr., 25/75, and 75/25 simulations. Additional hot spots occurred in the 119 lbs./hr. simulation at approximately 10", 42", 62", and 90" between 600–700 °C, 700–800 °C, 800–900 °C, and 900–1000 °C respectively.

Vertical and radial gradients were observed between the 900–1000 °C and 1000–1100 °C temperature regions in all the simulations, consistent with the previously discussed cooling profiles in section 3.1. In contrast, the 600–700 °C and 700–800 °C temperature regions exhibited vertical and radial gradients near the top and bottom of the canister but, only a radial gradient in the central part of the canister. The portion exhibiting no vertical gradient was estimated to occur between approximately 13" and 80" indicating that within this region the full radial cross section in the canister exhibited relatively constant heat flow as a function of time. In many of the simulations exhibiting radial gradients, the longest dwell times (for a given temperature region) occurred about the centerline as expected. This result was observed in the 228 lbs./hr. pour simulation and is fundamentally the basis for the current CCC. The most-uniform dwell time for the largest volumes of glass appeared to occur between 800 and 900 °C in most simulations as evidenced by the minimal gradients in those charts. Comparison of vertical and radial gradients indicates that the non-continuous simulations exhibited markedly similar behavior compared to the baseline albeit with clear discontinuities related to the simulation parameters.

To illustrate the effect of these temperature dwells, consider the baseline 228 lbs./hr. simulation dwell temperature charts shown in Figure 3-20. The maximum time that any portion of the glass remained between 800 and 900 °C was ~203 minutes. However, this portion of glass was a small portion (hot spot) of the entire glass volume. The majority of the glass volume appeared to remain between 800 and 900 °C for closer to ~ 160 minutes. Indeed, crystallization kinetics at the centerline compared to the surface of the canister may be significantly different. The various simulated temperature dwell times and associated locations indicate that the pour schedule can affect the heat flow in different parts of the canister in different ways.

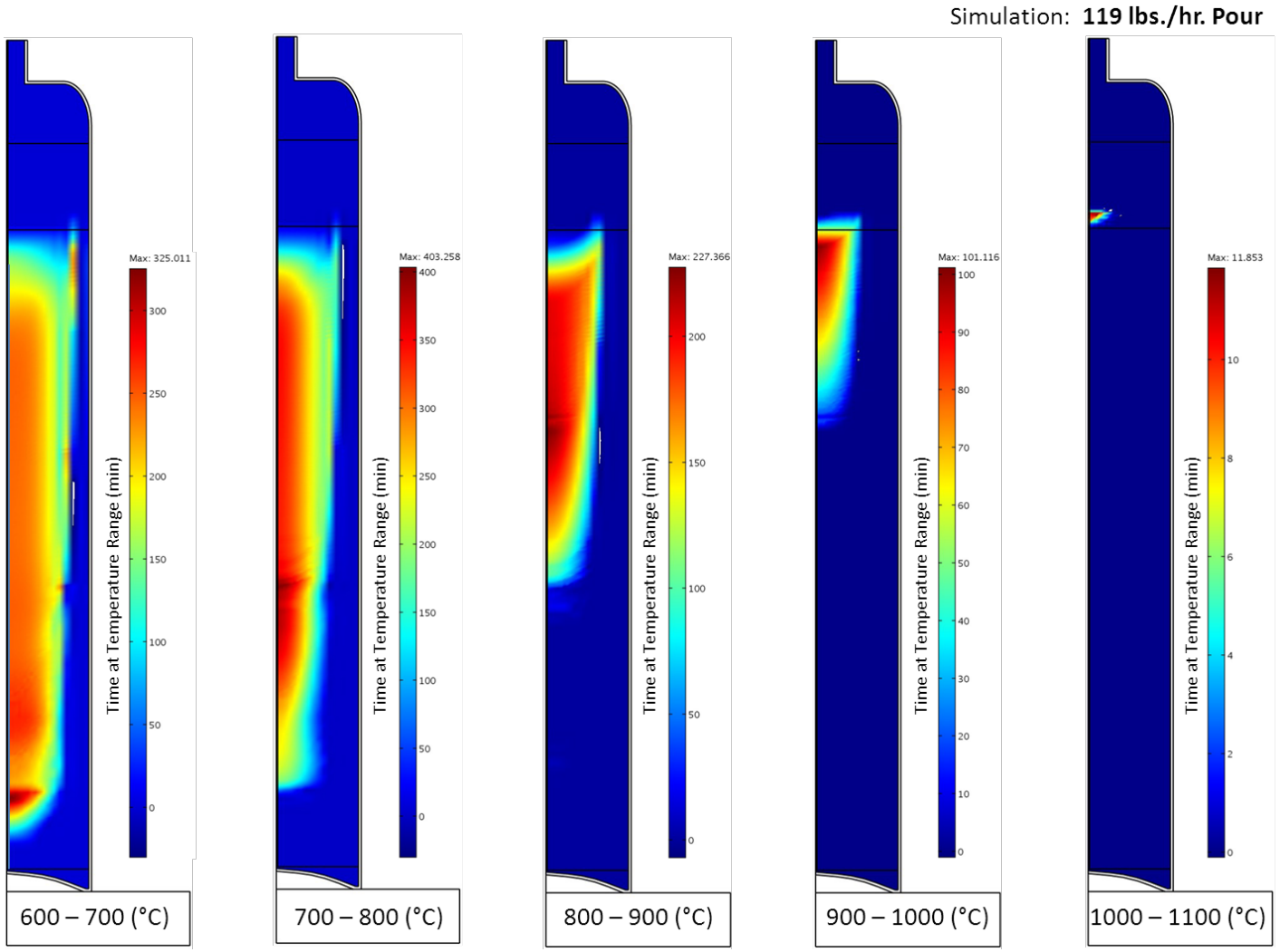

Figure 3-19. Temperature dwell charts for 119 lbs./hr. simulation. *Color represents the total time that portion of the glass was between the temperatures specified at the bottom of each chart. Scale ~ 25:1*

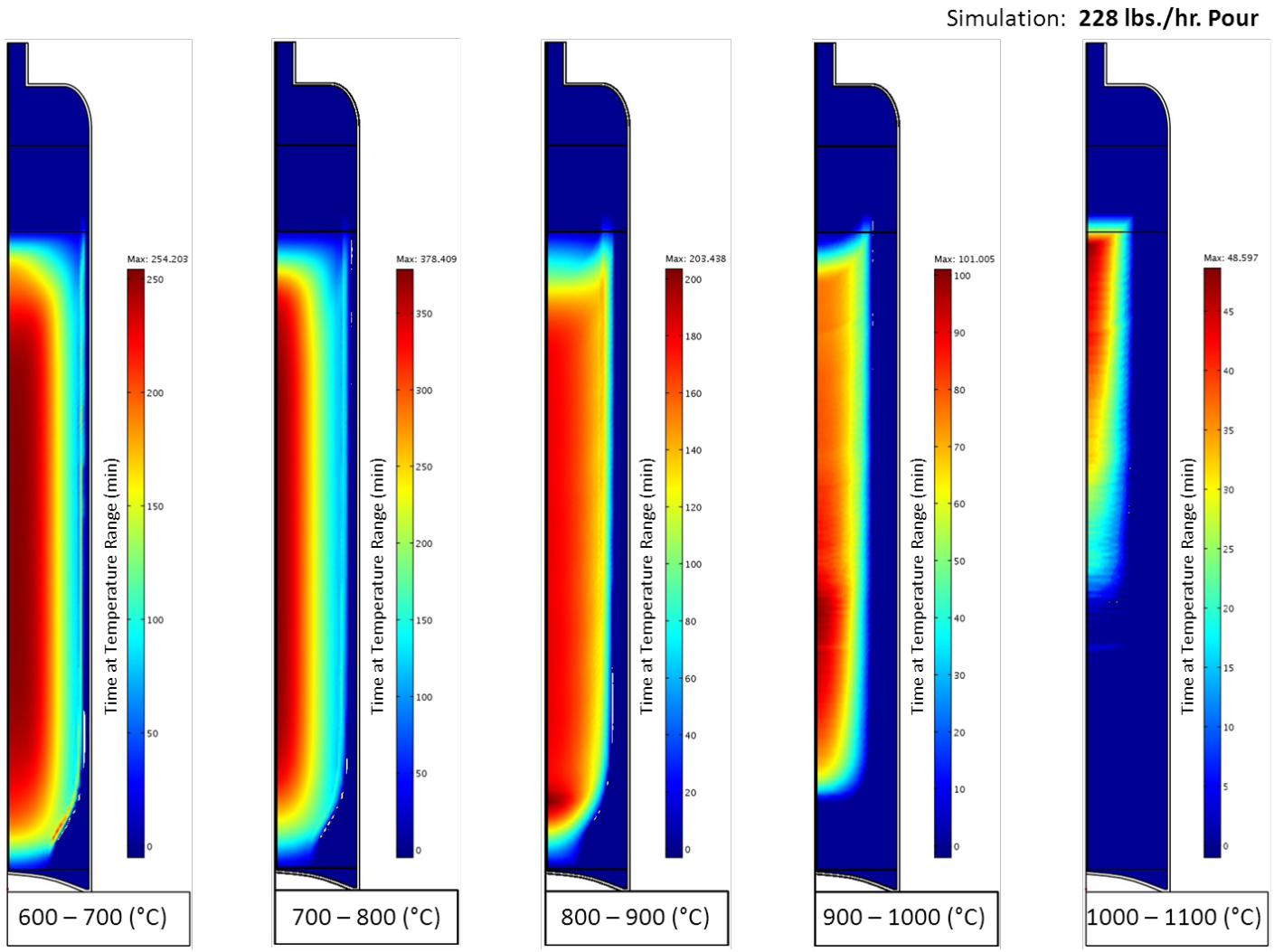

Figure 3-20. Temperature dwell charts for 228 lbs./hr. simulation. *Color represents the total time that portion of the glass was between the temperatures specified at the bottom of each chart. Scale ~ 25:1*

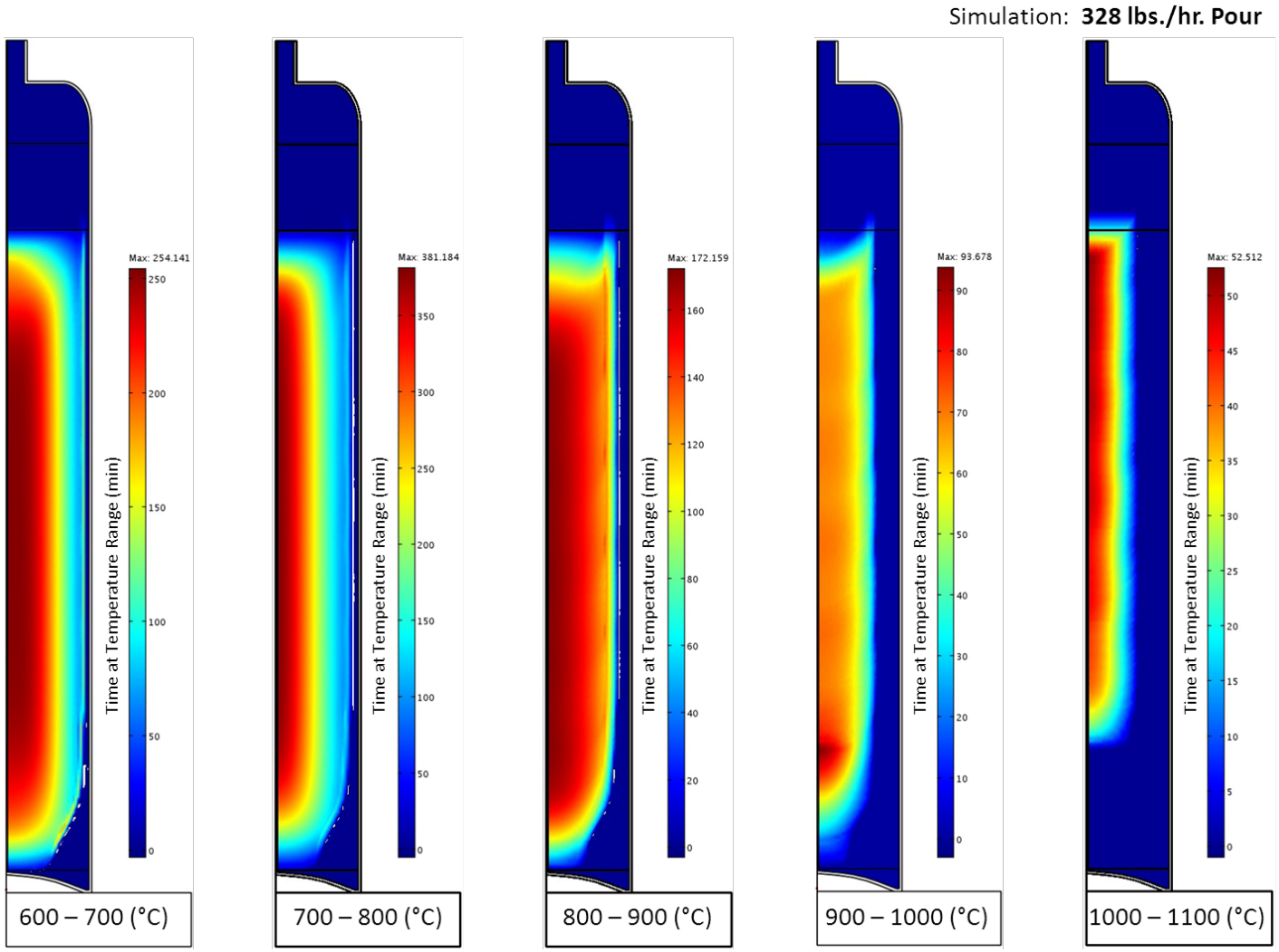

Figure 3-21. Temperature dwell charts for 328 lbs./hr. simulation. *Color represents the total time that portion of the glass was between the temperatures specified at the bottom of each chart. Scale ~ 25:1*

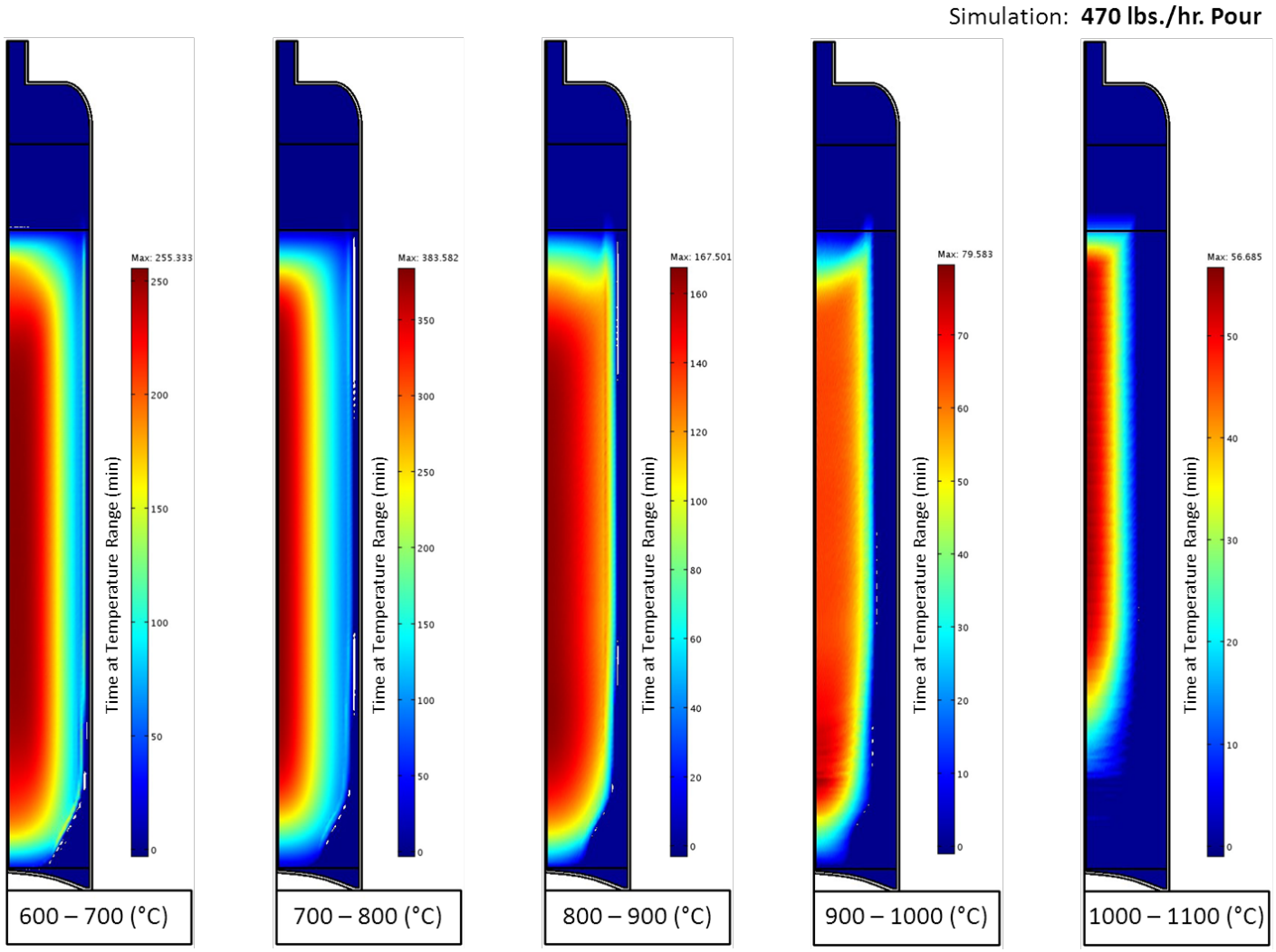

Figure 3-22. Temperature dwell charts for 470 lbs./hr. simulation. *Color represents the total time that portion of the glass was between the temperatures specified at the bottom of each chart. Scale ~ 25:1*

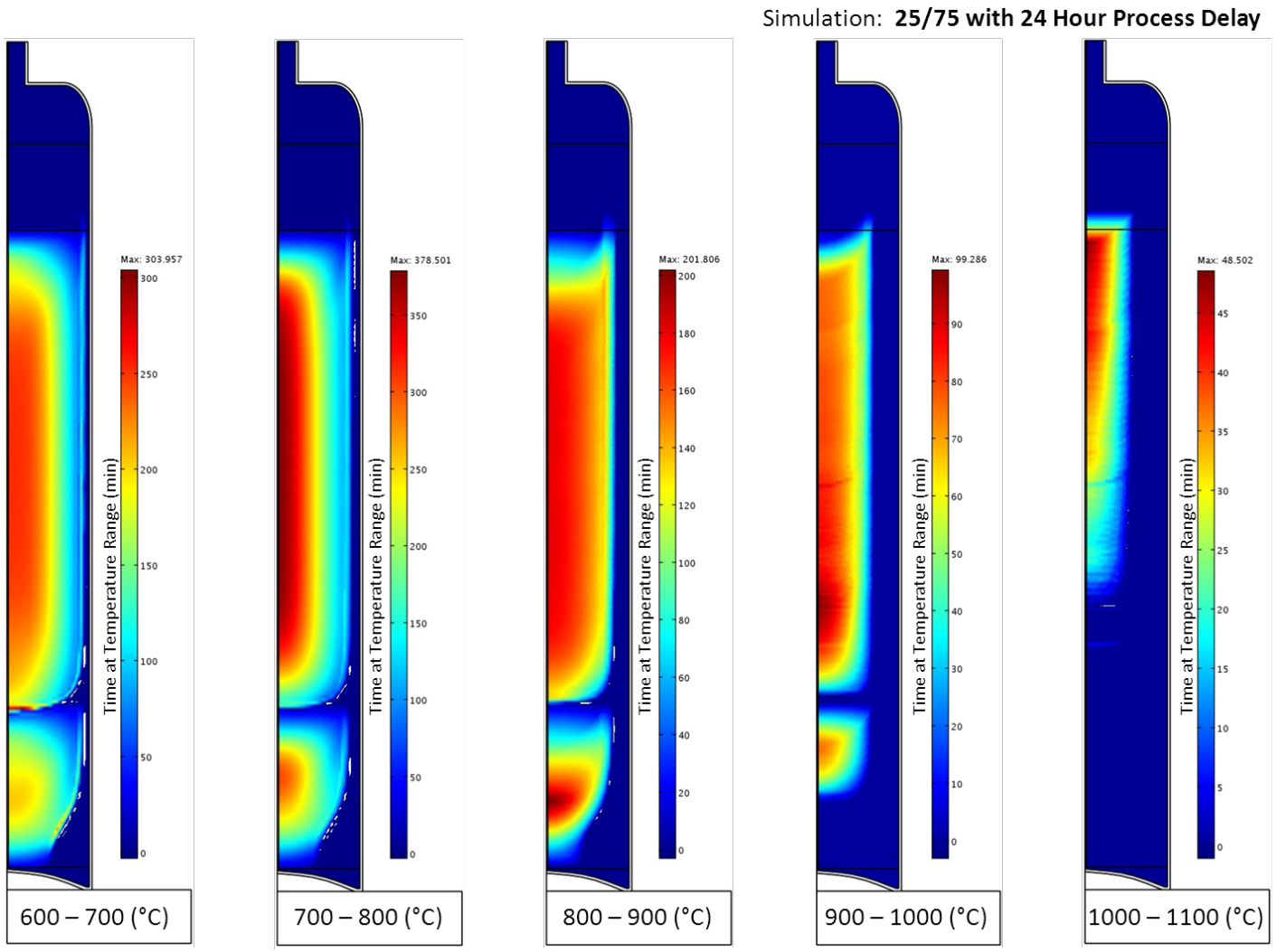

Figure 3-23. Temperature dwell charts for 25/75 with 24 hr. Process Delay simulation. *Color represents the total time that portion of the glass was between the temperatures specified at the bottom of each chart. Scale ~ 25:1*

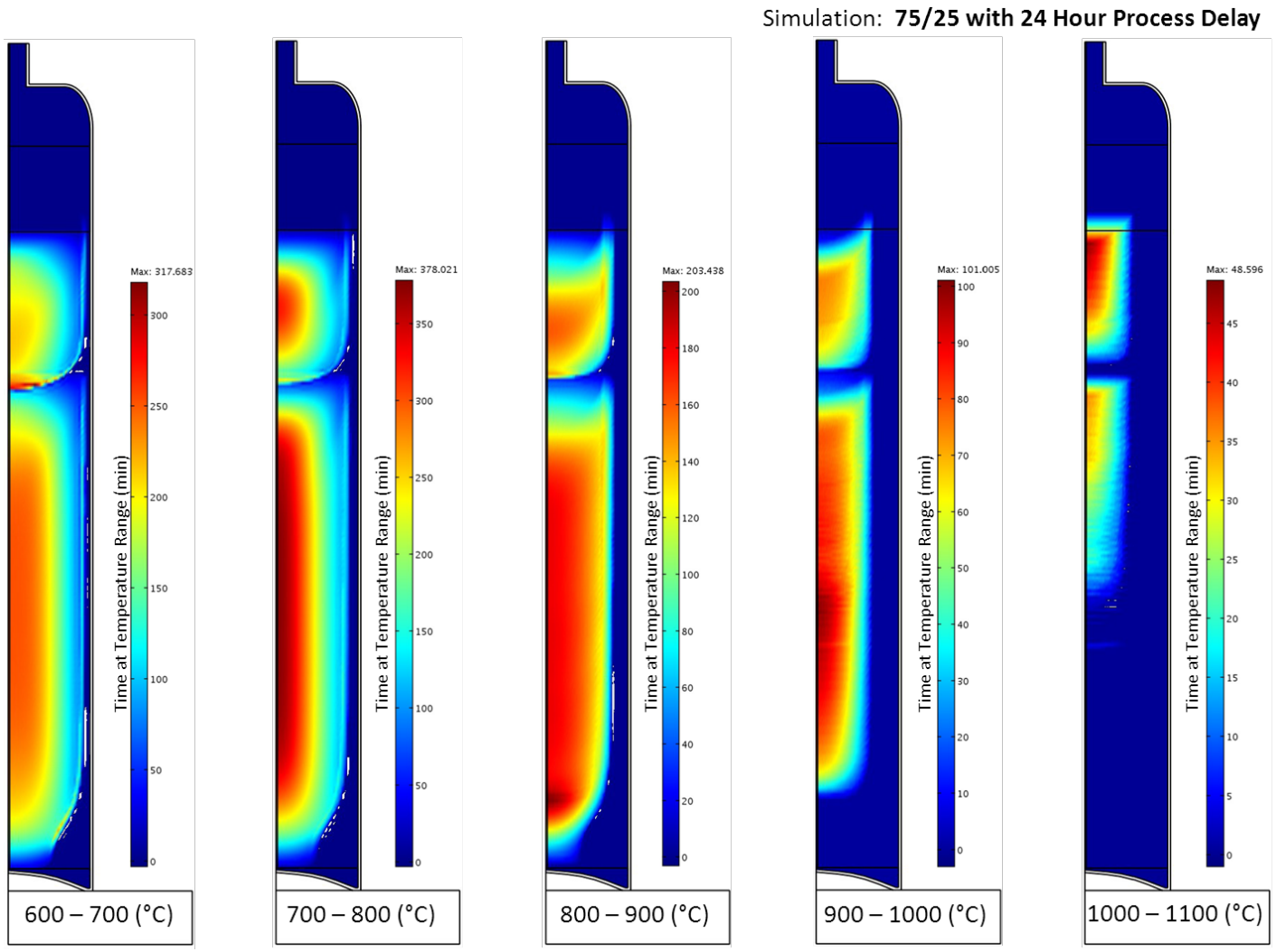

Figure 3-24. Temperature dwell charts for 75/25 with 24 hr. process delay simulation. *Color represents the total time that portion of the glass was between the temperatures specified at the bottom of each chart. Scale ~ 25:1*

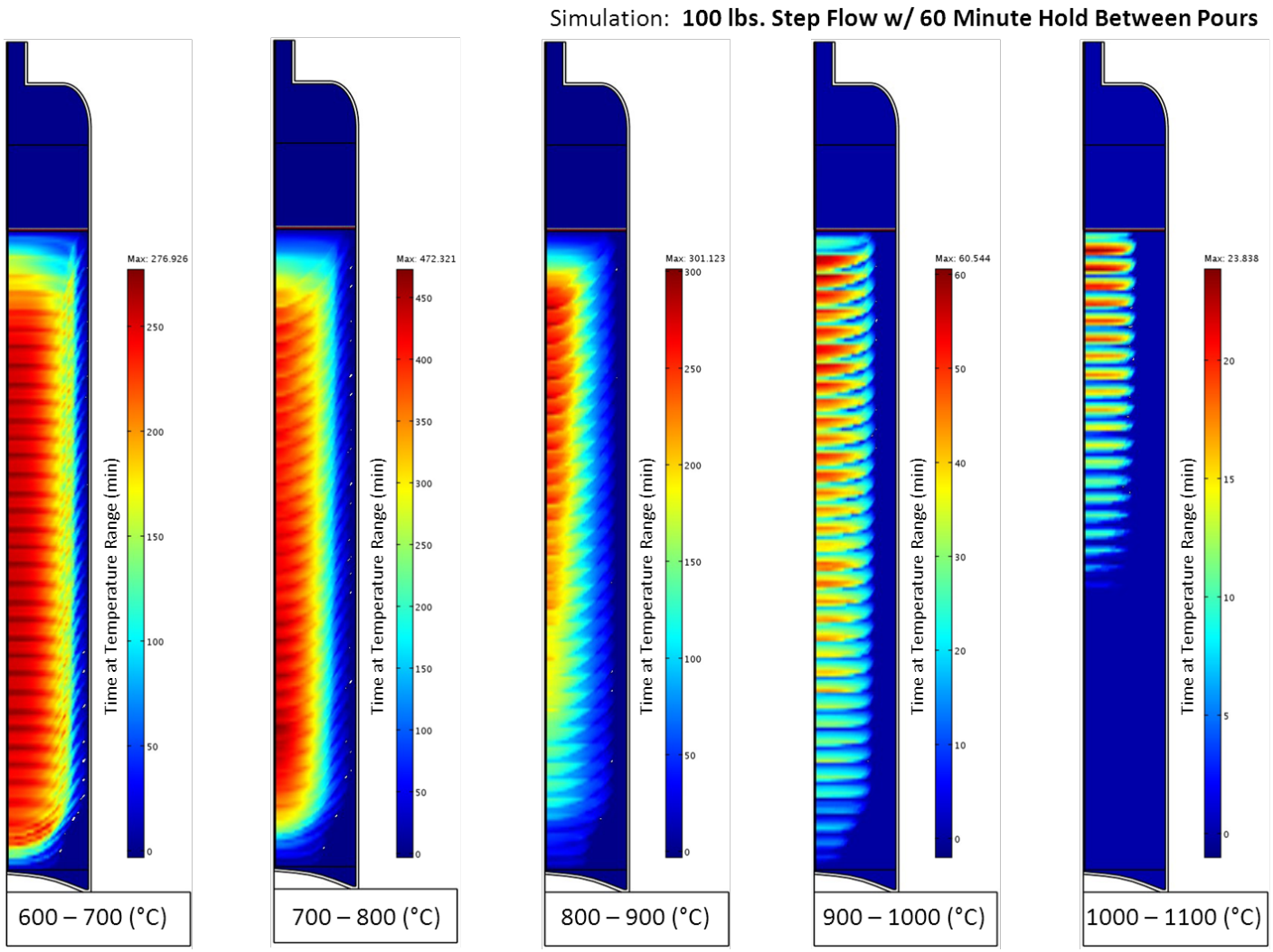

Figure 3-25. Temperature dwell charts for step flow with 100lbs./ 60 min. hold simulation. *Color represents the total time that portion of the glass was between the temperatures specified at the bottom of each chart. Scale ~ 25:11*

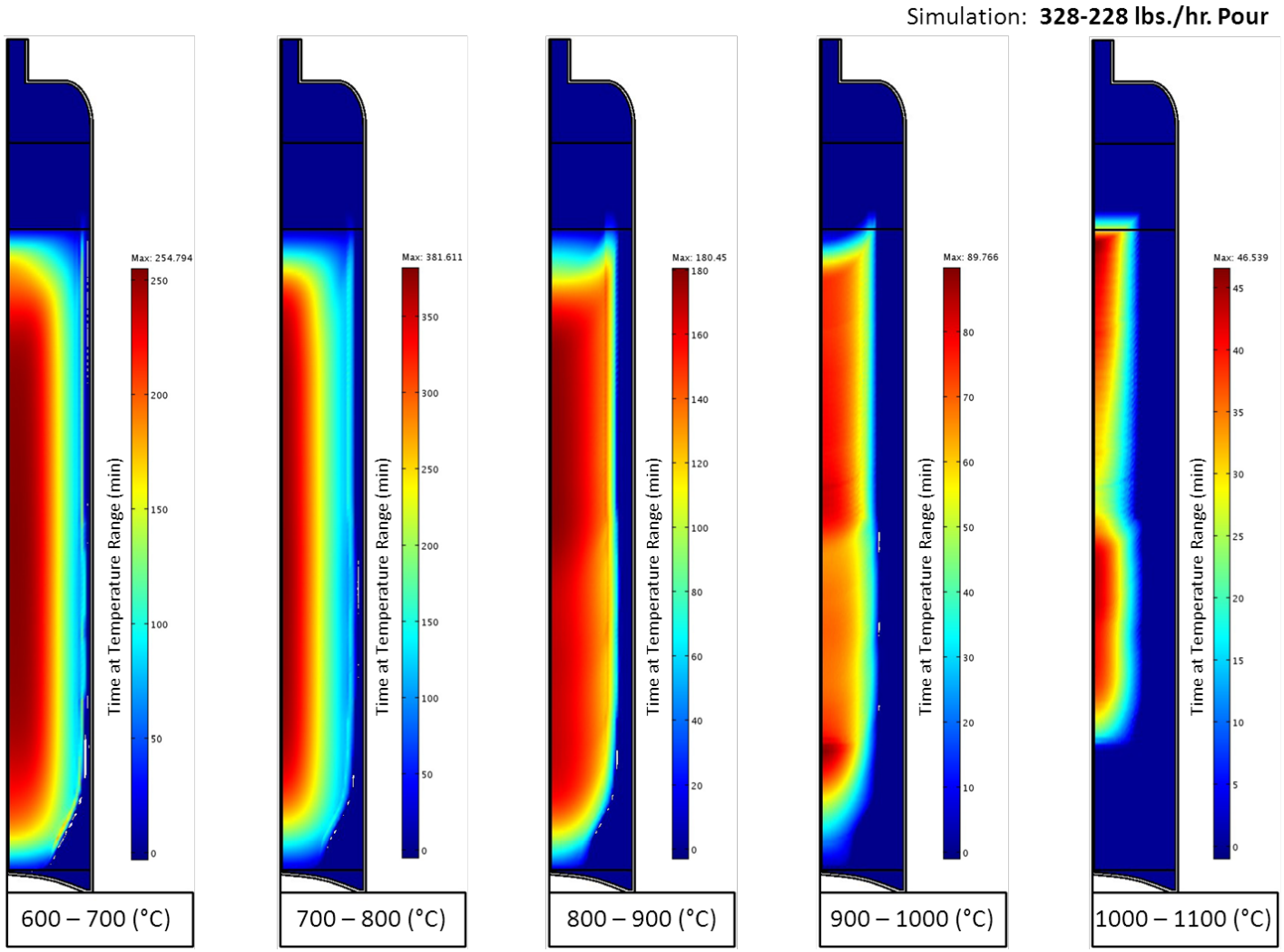

Figure 3-26. Temperature dwell charts for 328-228 lbs./hr. simulation. *Color represents the total time that portion of the glass was between the temperatures specified at the bottom of each chart. Scale ~ 25:1*

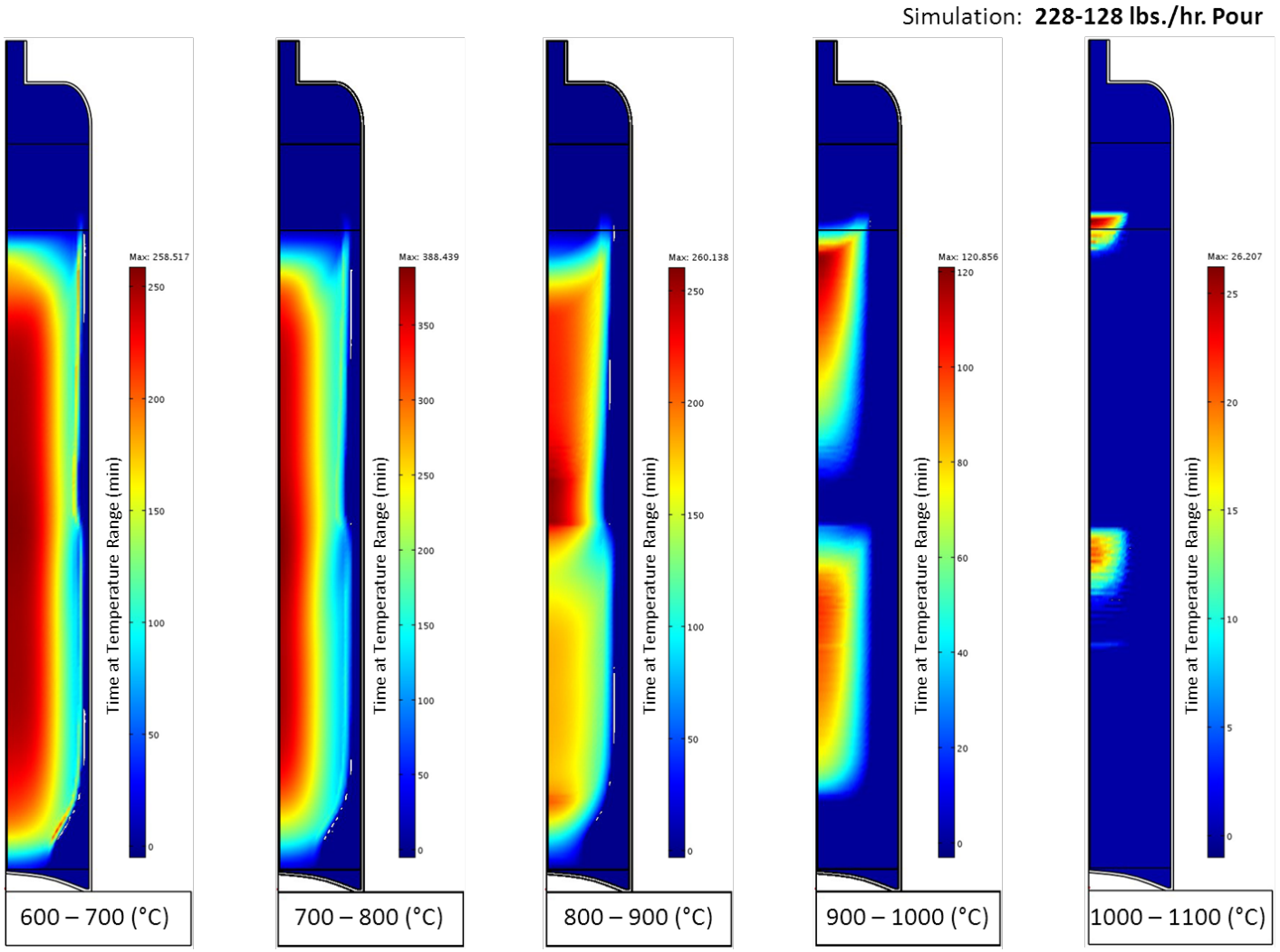

Figure 3-27. Temperature dwell charts for 228-128 lbs./hr. simulation. *Color represents the total time that portion of the glass was between the temperatures specified at the bottom of each chart. Scale ~ 25:11*

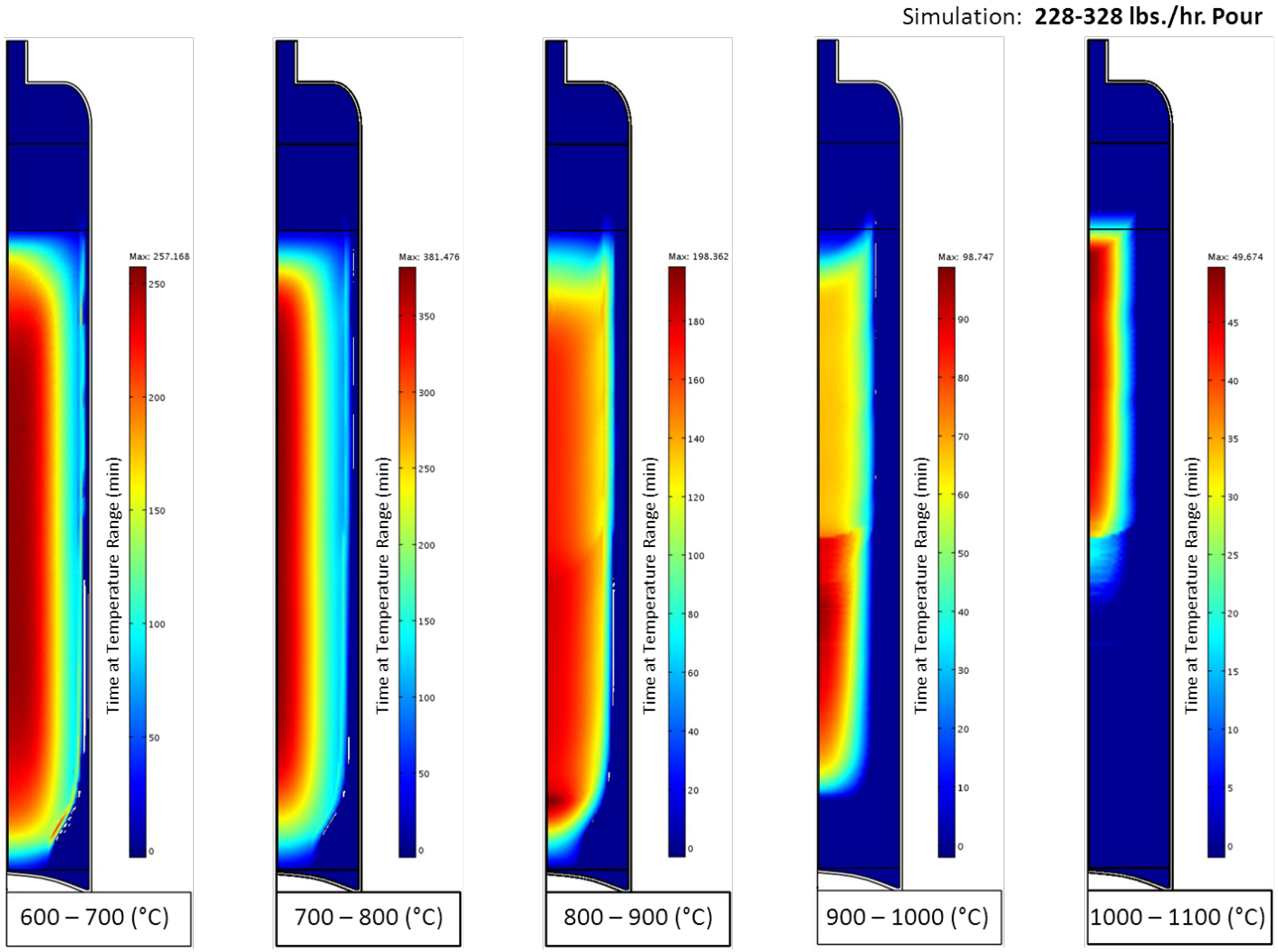

Figure 3-28. Temperature dwell charts for 228-328 lbs./hr. simulation. *Color represents the total time that portion of the glass was between the temperatures specified at the bottom of each chart. Scale ~ 25:11*

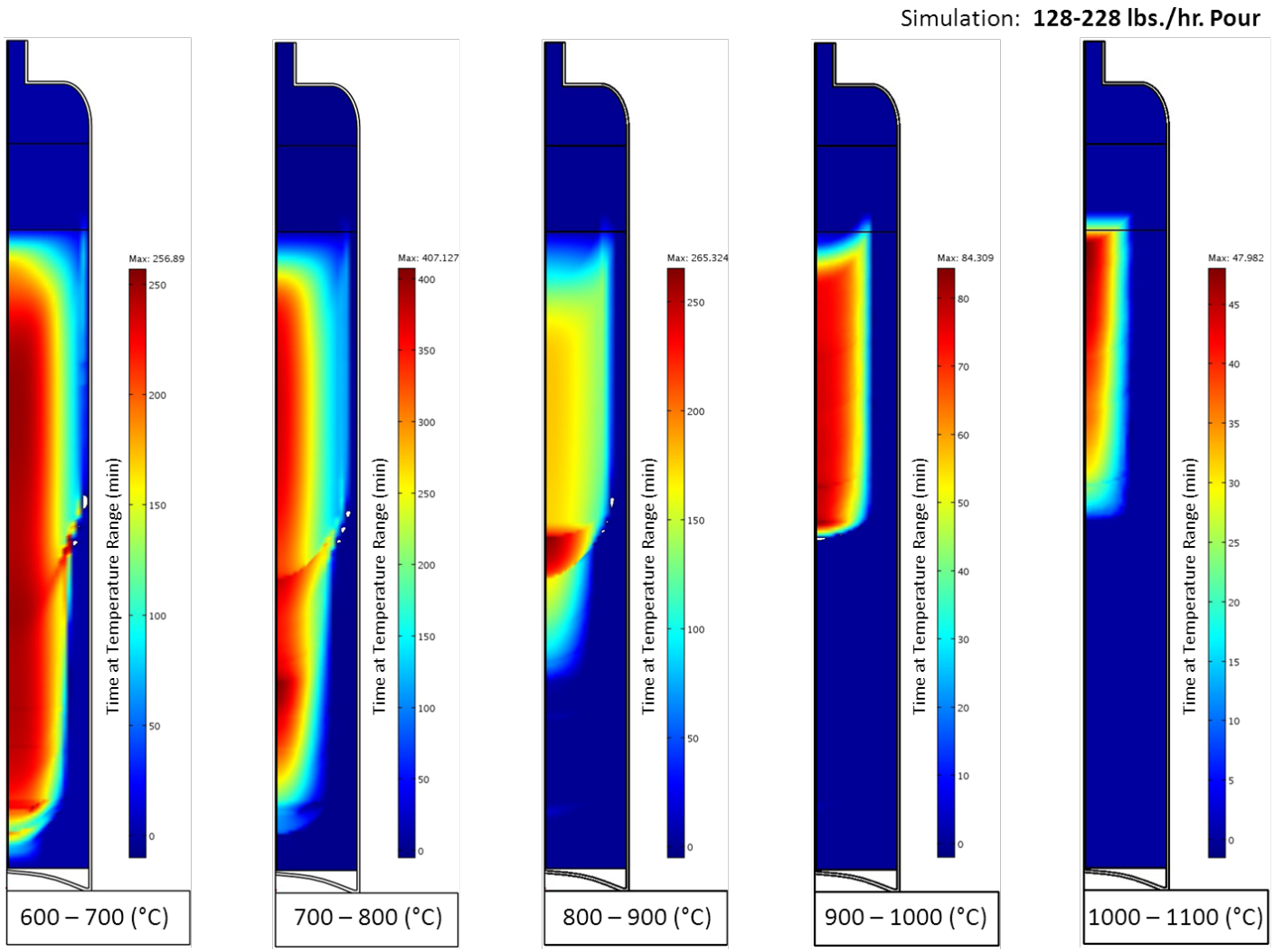

Figure 3-29. Temperature dwell charts for 128-228 lbs./hr. simulation. *Color represents the total time that portion of the glass was between the temperatures specified at the bottom of each chart. Scale ~ 25:11*

4.0 Summary

The study described here provided computer simulation data to supplement and advance the current understanding of, and ability to better predict, nepheline crystallization in HLW glasses. Results of the simulations indicate the pour rate can significantly impact the resultant temperatures and time that portions of HLW glass in DWPF canisters might be exposed to. Moreover, the simulations indicate that crystallization kinetics should not be expected to be uniform throughout the glass volume in a DWPF (or DWPF-like) canister and the simulations provide further evidence to the importance of considering the kinetics of nepheline formation when developing methods to predict and suppress its formation. To this point in particular, the CCC crucible test is thought to be conservative with respect to predicting nepheline formation. To elaborate, thermal (temperature) and chemical (interfacial) potentials will affect crystallization kinetics and therefore glass located at the center of the canister will have a different crystallization potential compared to that of glass located at the inside wall. Indeed, the CCC crucible test appears to artificially induce crystallization at the glass/crucible interface[a] due to the increased chemical driving force for crystallization at the surface compared to the center of the glass sample.[b] The implication is that nepheline crystallization is more likely to occur at the interface than in the bulk glass.[c] However, during processing of a DWPF canister, the cooling temperatures of the glass at the inside surface of the canister is significantly less compared to the glass at the interior (centerline) of the canister. It follows that the CCC crucible test would be conservative with respect to nepheline crystallization since the *thermal* driving force for crystallization would be larger than in an actual canister *at the surface*.[d]

The simulation results contain a tremendous amount of information useful in processing HLW glass that can be tailored to specific purposes for future studies. The glass properties, canister geometries, process parameters, etc. can be modified and simulations produced to evaluate the impact to the glass without actually filling a canister. Additionally, the simulations can be used as an investigative tool to easily and efficiently identify critical temperatures and cooling rates. In particular, experimental studies can be performed to identify the temperature regions in which nepheline crystallizes in HLW glass and then a simulation can be performed to rigorously identify or search for locations within the canister that are at increased risk. Subsequently, the simulation results can be used to develop precise laboratory tests to optimize glass formulations and processing parameters to avoid nepheline crystallization. Although the focus of this research is to gain a complete understanding of nepheline crystallization in HLW glass, the simulations need not be restricted in that sense. Indeed, other types of crystallization could be explored in similar ways.

[a] Similarly, the glass/air interface appears to lower the crystallization potential.
[b] The thermal driving force for crystallization is the same since the entire sample and crucible are exposed to the same cooling profile.
[c] It is possible that some glasses will not behave as described here, i.e. the interfacial driving forces may not be significantly different form the bulk driving forces. Also, the canister material is stainless steel and the CCC test is performed in Pt/Au alloy crucibles and interfacial effects may be different for different materials.
[d] Since the rates (as a function of temperature) of nepheline crystallization are not known this argument must be understood with caution. This argument does not suggest or imply the magnitude of crystallization potential. That is to say, a glass exposed to an alternative crucible test that utilized a *surface* cooling profile might still exhibit interface (glass/surface) crystallization. However, if interface crystallization was measured, the amount would be expected to be less than that compared to a glass exposed to the traditional CCC crucible test.

5.0 Path Forward

This research enforces the need to understand nepheline kinetics to optimize nepheline tolerance in HLW glasses. Nevertheless, further research is needed to holistically understand nepheline formation in HLW glasses. Three areas of focused research are suggested:

1) Glass-surface interface effects–It has been shown that nepheline crystallization in HLW glass is dominated by surface/interface crystallization in the CCC crucible test.[6] The CCC test is currently performed in Pt/Au alloy crucibles. Experiments to determine the effect of different materials, specifically the canister material, on crystallization should be performed.

2) Nepheline nucleation and crystallization–The nucleation and crystal growth rates as a function of temperature need to be experimentally determined for typical HLW glass compositions in order to develop alternative methods to avoid crystallization.

3) Laboratory crucible tests–It now seems apparent given the data to date, that the current CCC crucible test is likely conservative. Experimental work should focus on developing laboratory tests to more accurately mimic the cooling profile of the glass in canister that is at most risk to nepheline crystallization.

It is vital to communicate to the reader that the preceding recommendations are interdependent and need to be addressed collectively in order to draw *appropriate* conclusions. Subsequently, a determination can be made whether the ND as implemented has been overly conservative. Then the use of the CCC and the waste compliance strategy can be modified as necessary.

6.0 References

1. H. Li, J. D. Vienna, P. Hrma, D. E. Smith and M. J. Schweiger, "Nepheline Precipitation in High-Level Waste Glasses: Compositional Effects and Impact on the Waste Form Acceptability," *Materials Research Soc. Symp. Proc.*, **465** pp. 261-68, (1997).

2. T. B. Edwards, D. K. Peeler and K. M. Fox, "The Nepheline Discriminator: Justification and DWPF PCCS Implementation Details," *U.S. Department of Energy Report WSRC-STI-2006-00014,* Aiken, SC (2006).

3. J. R. Fowler, R. E. Edwards, S. L. Marra and M. J. Plodinec, "Chemical Compostion Projections for the DWPF Product," *WSRC-IM-91-116-1 Revision 1, Part 3 Item 100,* Westinghouse Savannah River Company, Aiken, SC (1995).

4. K. A. Hauer, "DWPF Waste Form Compliance Plan," *WSRC-IM-116-0 Revision 8,* Aiken, SC (2006).

5. S. L. Marra and C. M. Jantzen, "Characterization of Projected DWPF Glasses Heat Treated to Simulate Centerline Cooling," *US Department of Energy Report WSRC-TR-92-142, Revision 1,* Westinghouse Savannah River Company, Aiken, SC (1993).

6. J. W. Amoroso, "The Impact of Kinetics on Nepheline Formation in Nuclear Waste Glasses," *US Department of Energy Report SRNL-STI-2011-00051,* Savannah River National Laboratory, Aiken, SC (2011).

7. J. W. Amoroso, "Nepheline Nucleation and Crystal Growth In Waste Glasses: Interim Report " *US Department of Energy Report SRNL-STI-2011-00549,* Savannah River National Laboratory, Aiken, SC (2011).

8. EM-30 Technology Development and Deployment (TDD) Program Task Plan, "Task Plan for WP-5 Task 5.1.2 Advanced Silicate Glass Development and Demonstration," *WP5-5.1.2-FY2011 Revision 0*, (2011).

9. M. R. Kesterson, "COMSOL Multiphysics Model for DWPF Canister Filling," *US Department of Energy Report SRNL-STI-2011-00209 Revision 1,* Savannah River National Laboratory, Aiken, SC (2011).

10. R. E. Edwards, "SGM 8 - Canister and Glass Temperatures During Filling and Cooldown," *Inter-Office Memorandum DPST-87-801*, Westinghouse Savannah River Company, Aiken, SC (1987).

11. M. H. Tennant, "Thermal Analysis of DWSF Canister Processing," *Interoffice Memorandum DPST-78-00380*, Aiken, SC (1978).

12. D. J. Pellarin, "DWPF Canister & Glass Temperatures During Filling & Cooldown," *DPST-85-954,* Technical Division, Savannah River Laboratory, Aiken, SC (1985).

13. Personal Communication with A. B. Barnes. Aiken, SC,

14. COMSOL Inc., *COMSOL Multiphysics*, *3.5a*, Burlington, MA.

15. D. P. Chew and B. A. Hamm, "Liquid Waste System Plan," *SRR-LWP-2009-00001, Revision 16,* Aiken, SC (20110).

16. C. A. Cicero, S. L. Marra and M. K. Andrews, "Phase Stability Determinations of DWPF Waste Glasses," *US Department of Energy Report WSRC-TR-93-227, Rev. 0,* Westinghouse Savannah River Company, Aiken, SC (1993).

17. D. Missimer, A. Jurgensen and R. Rutherford, "High Temperature X-ray Diffraction Analyses of NP2-14, NP2-18, and NP2-24 Glasses in He Following the Center-Lined Cooling Curve Protocol," *U.S. Department of Energy Report SRNL-L4200-2009-00006,* Savannah River National Laboratory, Aiken, SC (2009).

18. J. P. Holman, "Heat Transfer," 2nd Edition. McGraw-Hill, 1968.

Appendix A.

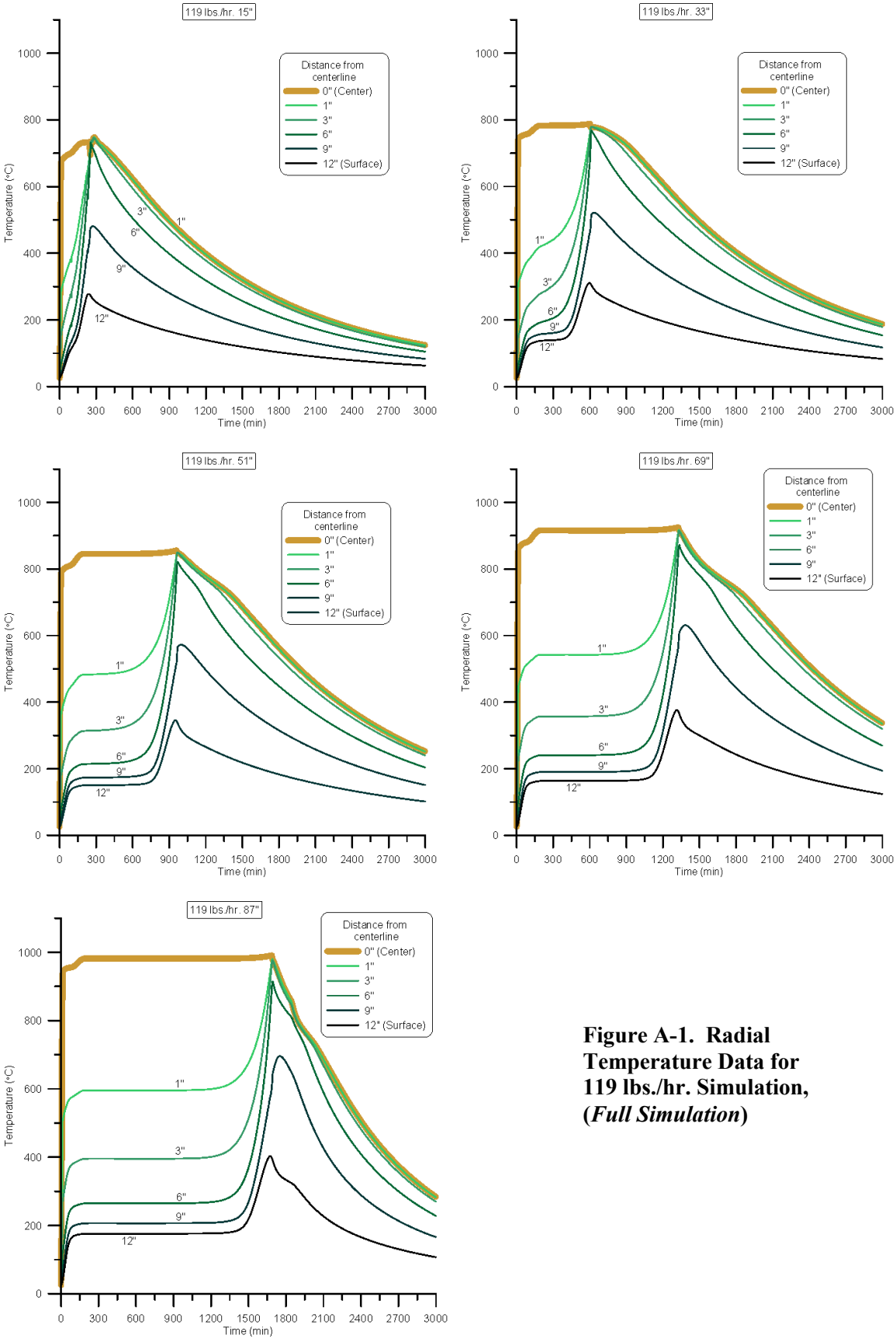

Figure A-1. Radial Temperature Data for 119 lbs./hr. Simulation, (*Full Simulation*)

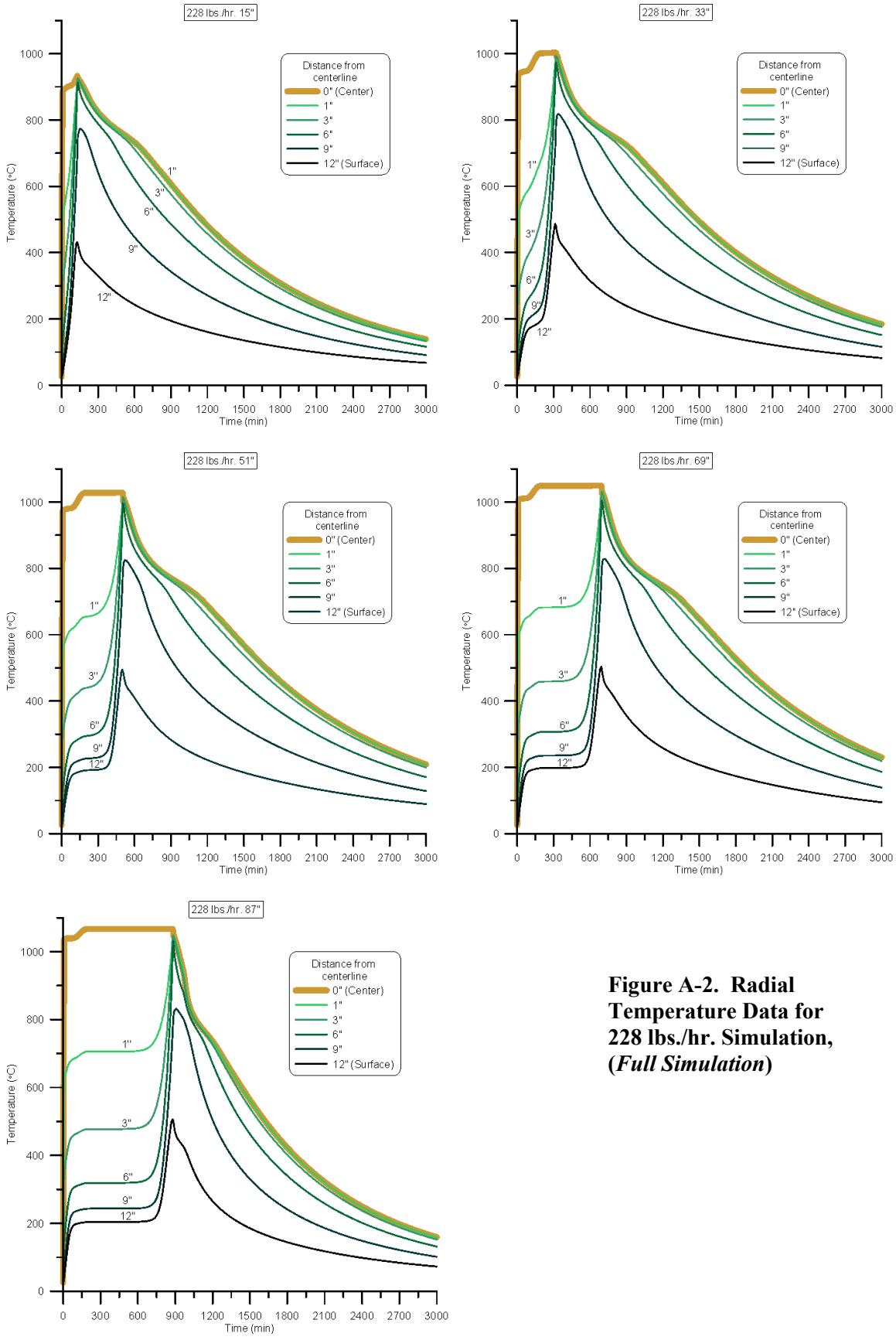

Figure A-2. Radial Temperature Data for 228 lbs./hr. Simulation, (*Full Simulation*)

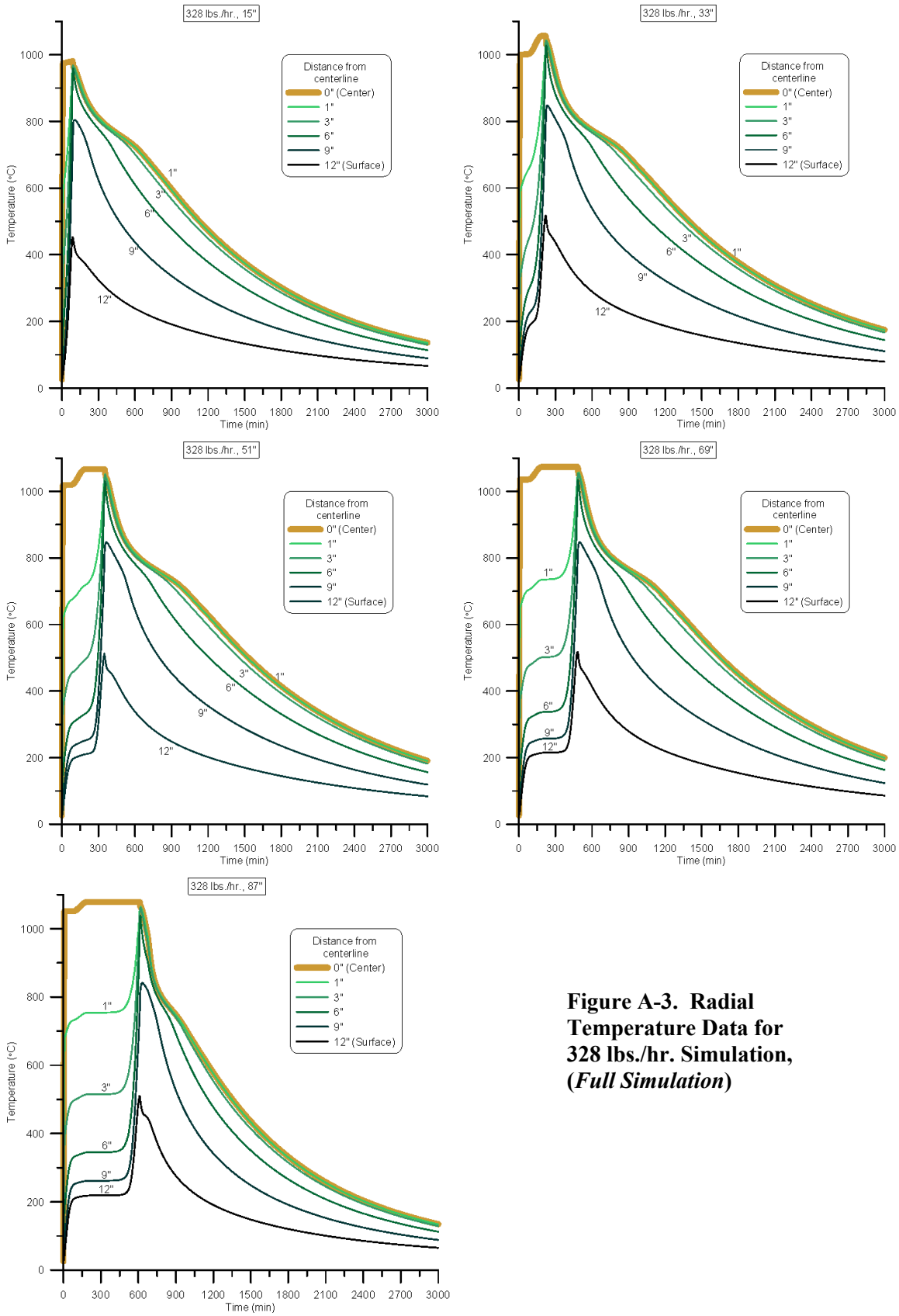

Figure A-3. Radial Temperature Data for 328 lbs./hr. Simulation, (*Full Simulation*)

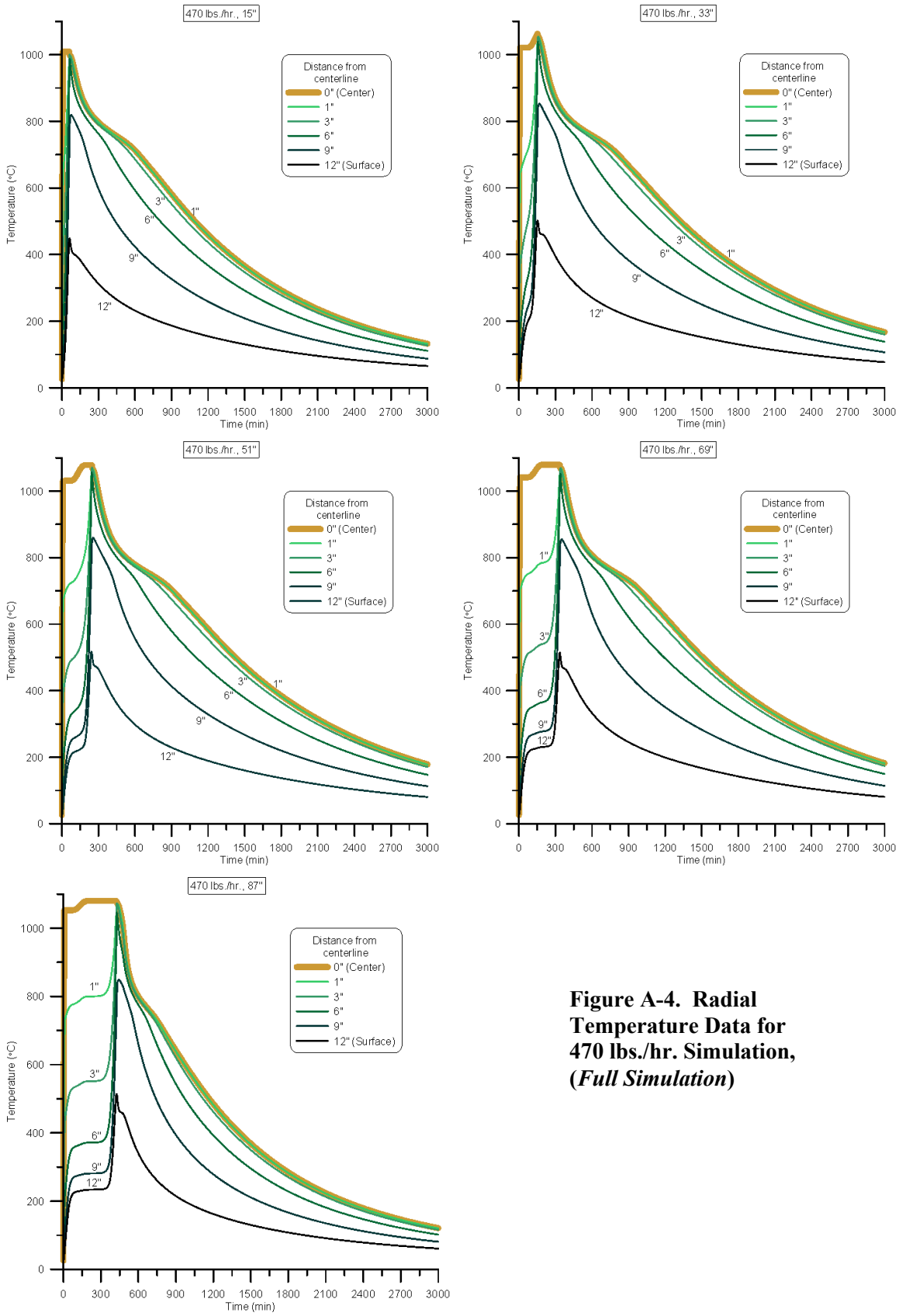

Figure A-4. Radial Temperature Data for 470 lbs./hr. Simulation, (*Full Simulation*)

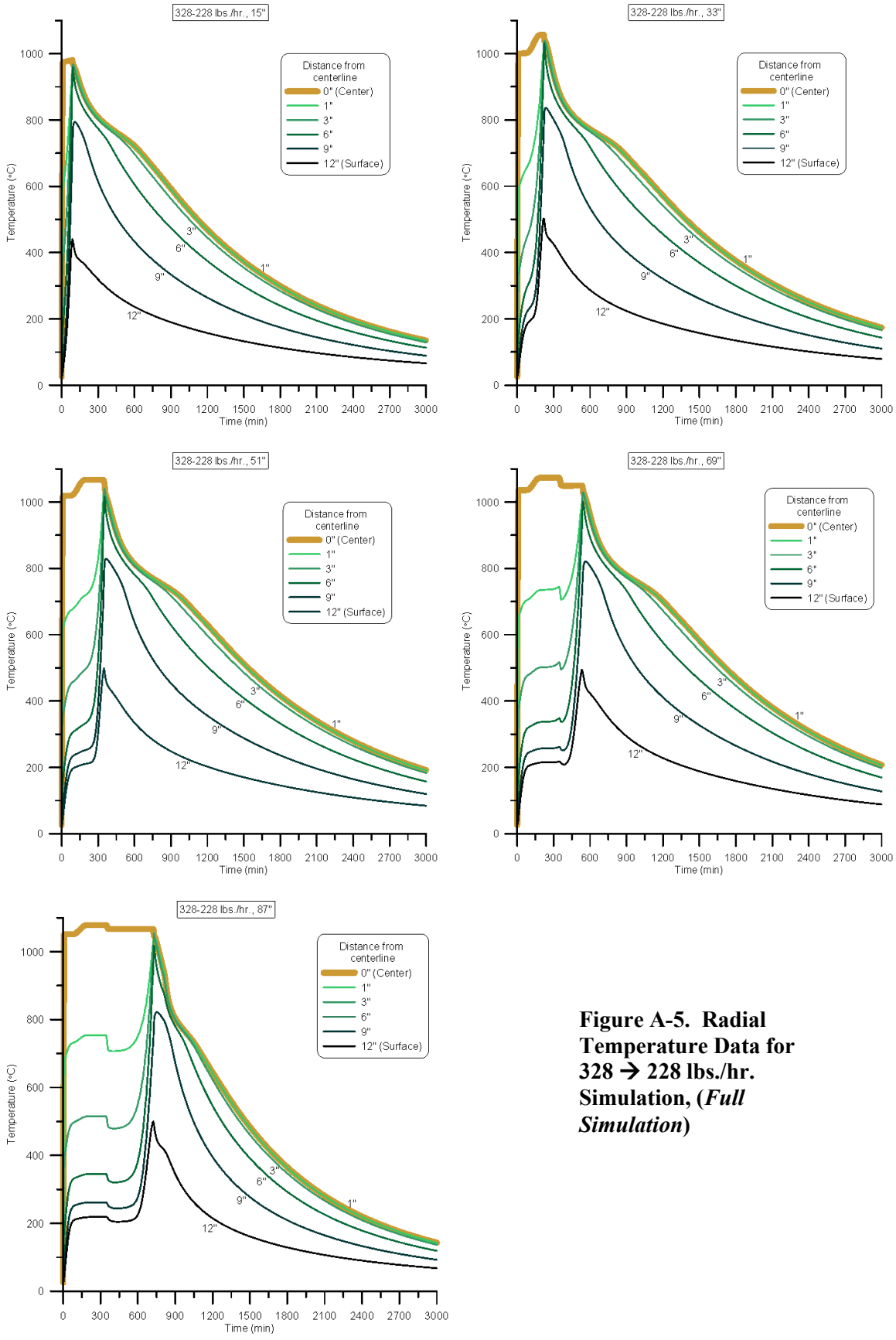

Figure A-5. Radial Temperature Data for 328 → 228 lbs./hr. Simulation, (*Full Simulation*)

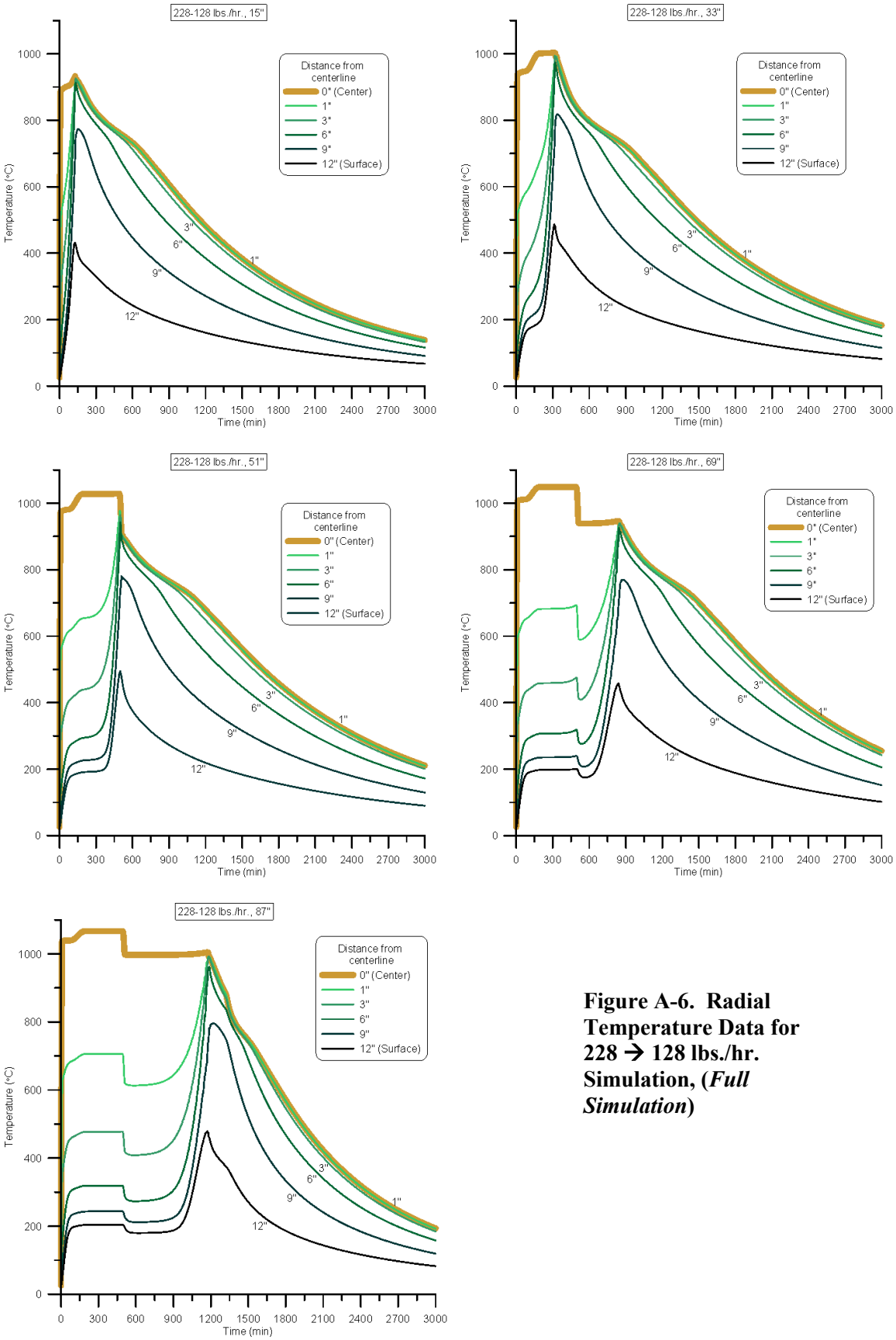

Figure A-6. Radial Temperature Data for 228 → 128 lbs./hr. Simulation, (*Full Simulation*)

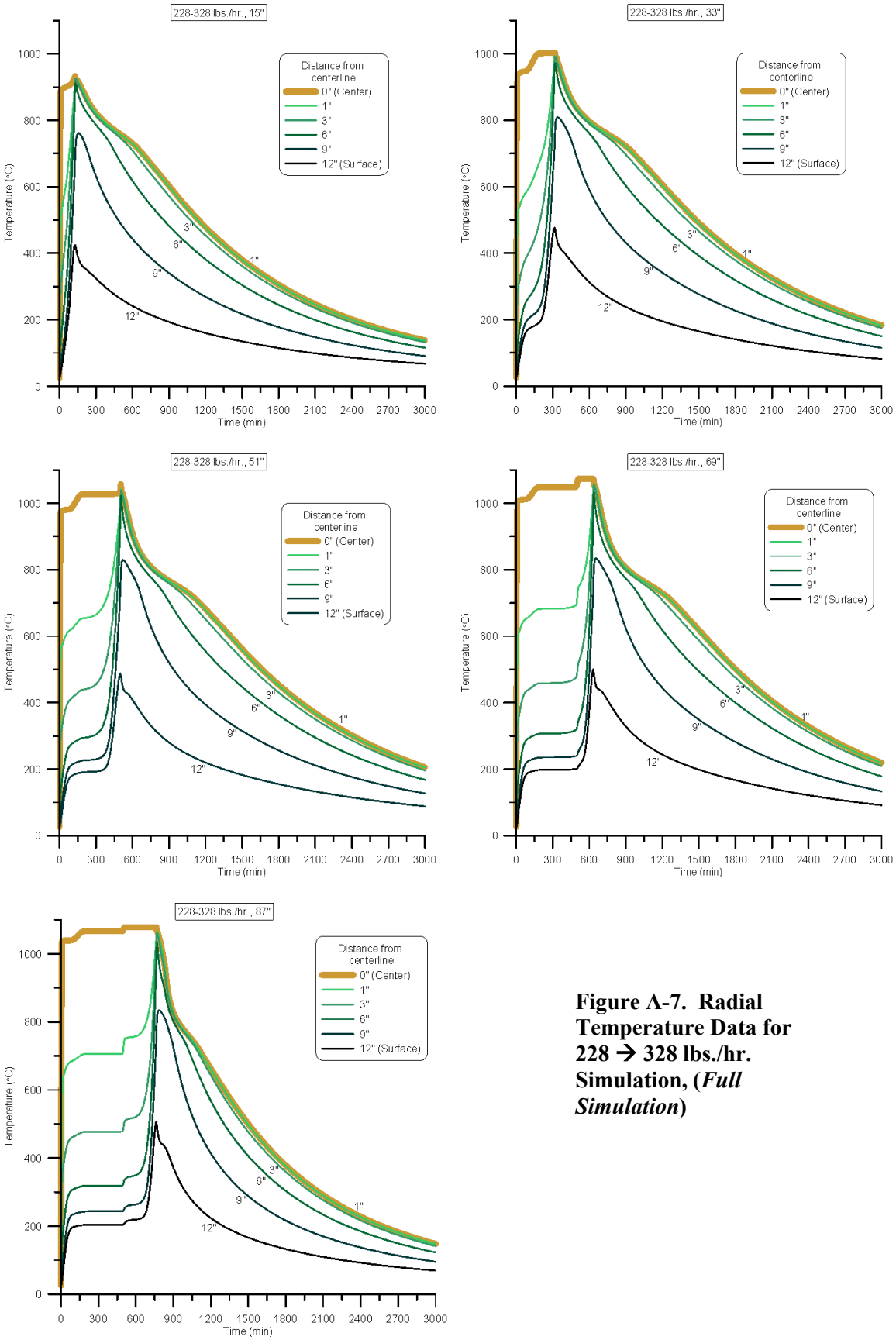

Figure A-7. Radial Temperature Data for 228 → 328 lbs./hr. Simulation, (*Full Simulation*)

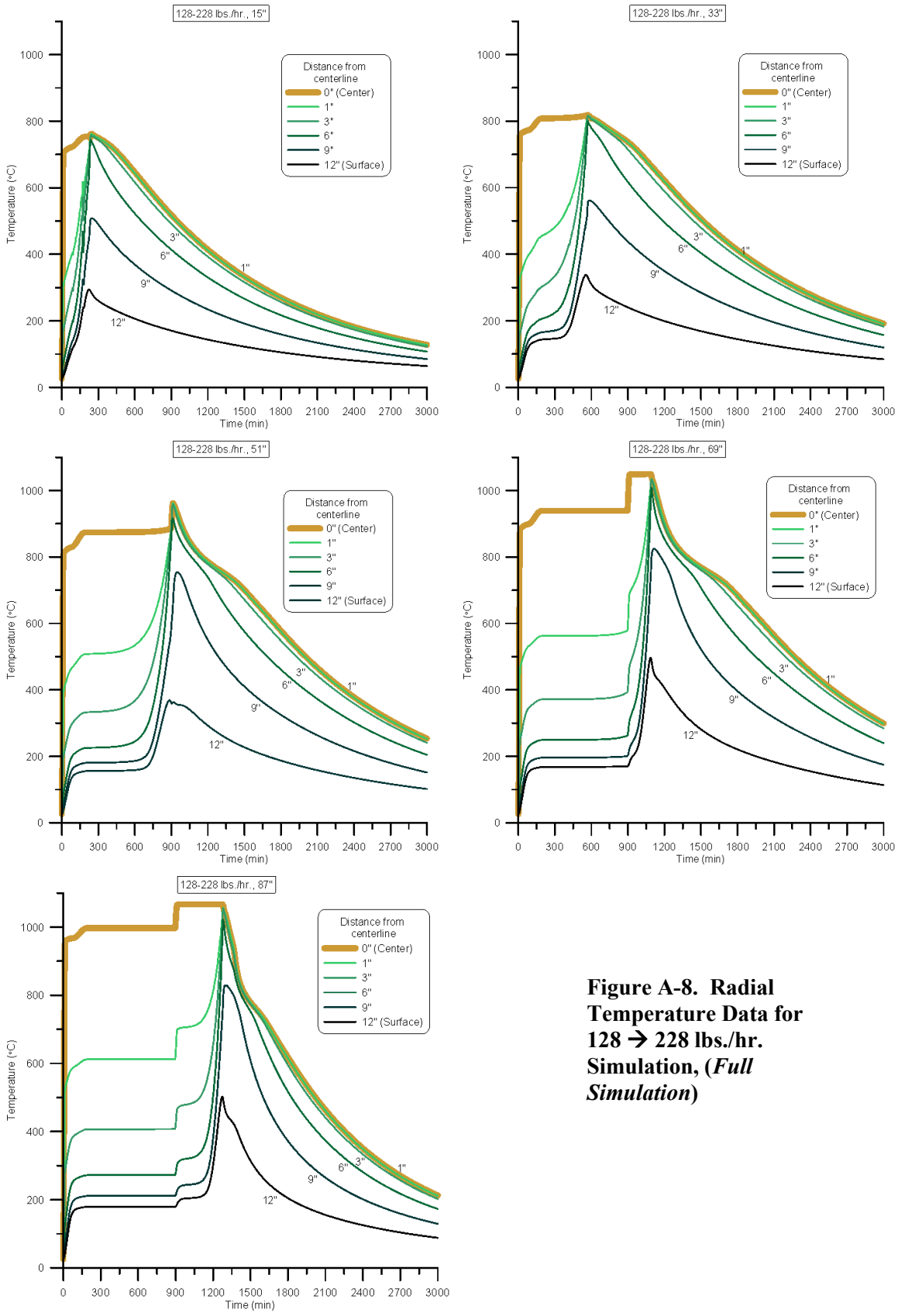

Figure A-8. Radial Temperature Data for 128 → 228 lbs./hr. Simulation, (*Full Simulation*)

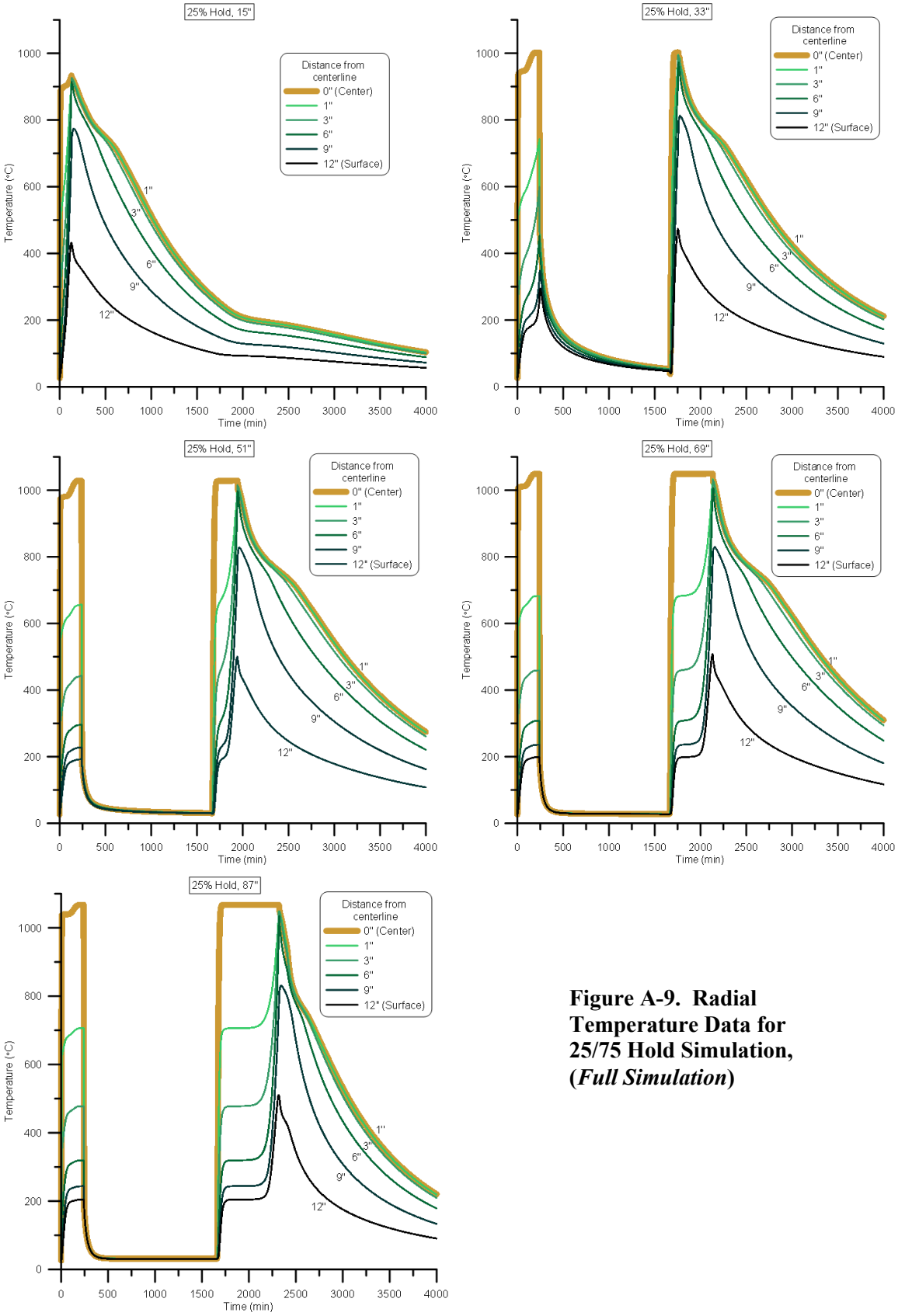

Figure A-9. Radial Temperature Data for 25/75 Hold Simulation, (*Full Simulation*)

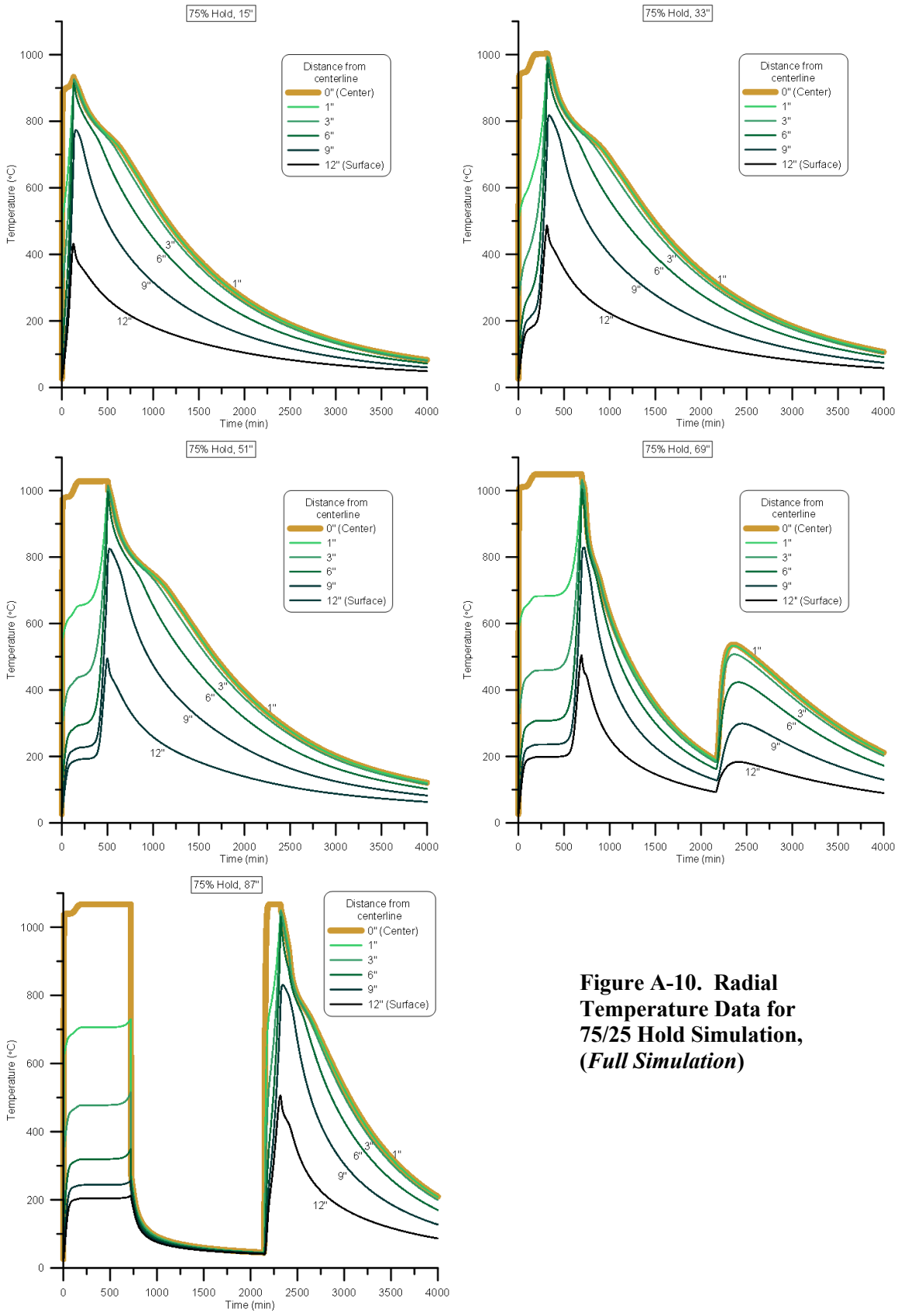

Figure A-10. Radial Temperature Data for 75/25 Hold Simulation, (*Full Simulation*)

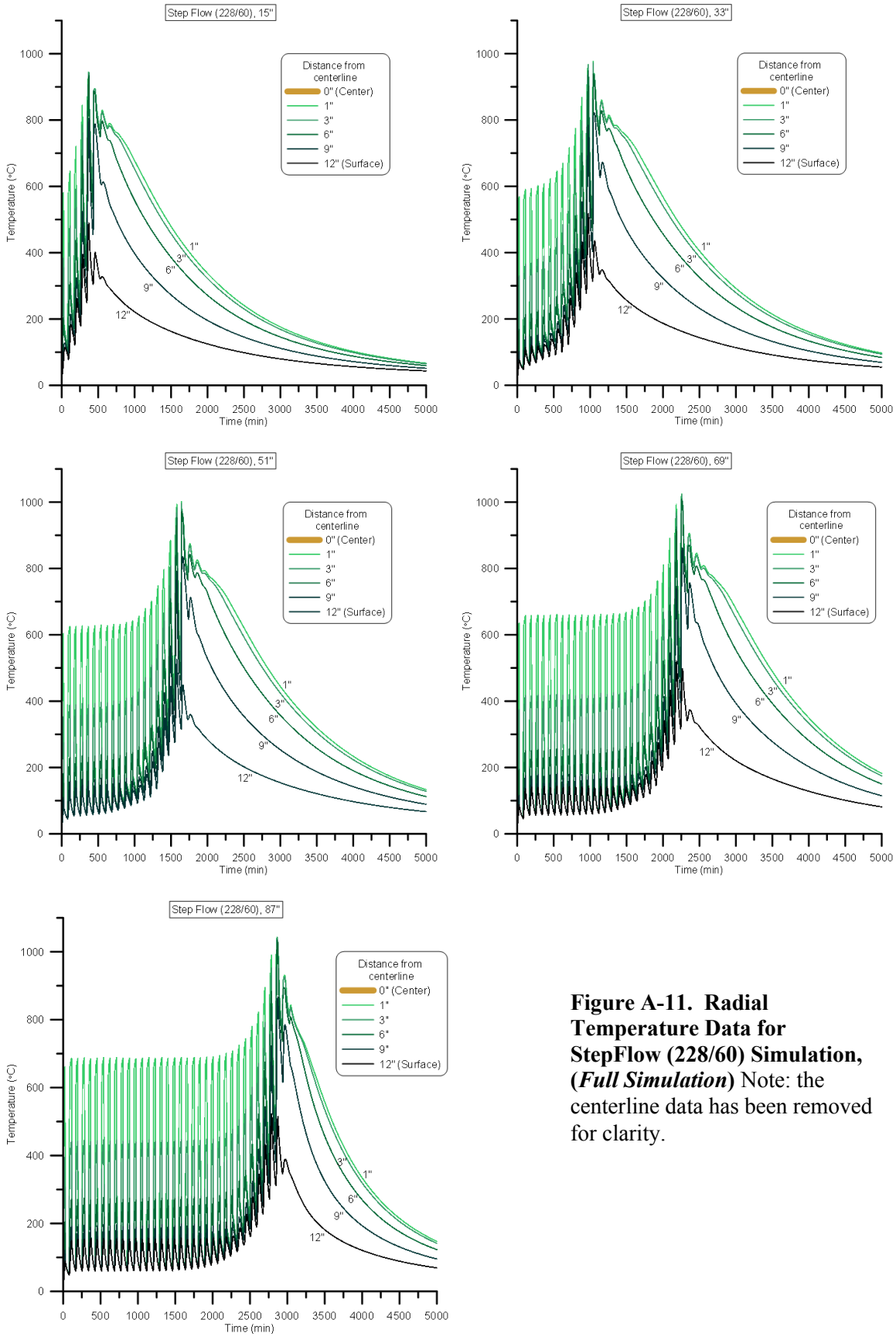

Figure A-11. Radial Temperature Data for StepFlow (228/60) Simulation, (*Full Simulation*) Note: the centerline data has been removed for clarity.

Distribution:

J. W. Amoroso, 999-W
A. B. Barnes, 999-W
C. L. Crawford, 773-42A
D. A. Crowley, 773-43A
A. P. Fellinger, 773-41A
S. D. Fink, 773-A
K. M. Fox, 999-W
B. J. Giddings, 786-5A
C. C. Herman, 999-W
J. F. Iaukea, 704-30S
C. M. Jantzen, 773-A
F. C. Johnson, 999-W
S. L. Marra, 773-A
J. E. Occhipinti, 704-S
D. K. Peeler, 999-W
F. M. Pennebaker, 773-42A
J. W. Ray, 704-S
D. C. Sherburne, 704-S
M. E. Smith, 704-30S
A. V. Staub, 704-27S
M. E. Stone, 999-W
W. R. Wilmarth, 773-A